THESIS

THE GEOLOGY OF THE TRACY CANYON AREA, SAGUACHE COUNTY, COLORADO

Submitted by

James W. Newman

In partial fulfillment of the requirements

for the Degree of Master of Science

Colorado State University

Fort Collins, Colorado

Spring, 1976

COLORADO STATE UNIVERSITY

Spring, 1976

WE HEREBY RECOMMEND THAT THE THESIS PREPARED UNDER OUR SUPERVISION BY JAMES W. NEWMAN ENTITLED THE GEOLOGY OF THE TRACY CANYON AREA, SAGUACHE COUNTY, COLORADO BE ACCEPTED AS FULFILLING IN PART REQUIREMENTS FOR THE DEGREE OF MASTER OF SCIENCE.

Committee on Graduate Work

Larry K. Burns

C. G. Warren

M. E. McCallum

Jimmy B. Thompson
Adviser

Theodore Chamberlain
Head of Department

ABSTRACT OF THESIS

THE GEOLOGY OF THE TRACY CANYON AREA,
SAGUACHE COUNTY, COLORADO

The study area encompasses approximately 30 square kilometers in the Laughlin Gulch and Saguache, Colorado Quadrangles about 13 kilometers southwest of the town of Saguache. Conejos Formation volcanics of the "early intermediate assemblage" as described by Lipman et al. (1970), are mapped as four separate flow units. Pyroclastic rocks, representatives of the second major episode of San Juan volcanism, are absent in the study area. The Conejos Formation volcanics are partially capped by olivine basaltic andesites of the Hinsdale Formation, and represent the "late bimodal eruptive episode." Intrusives in the area represent all of the major volcanic episodes of the northeastern San Juan Mountains.

Flows in the study area are commonly tilted gently to the northeast in response to regional deformation associated with development of the Rio Grande block fault system. Faults are expressed as valleys and topographic breaks. They tend to be short or gently curved and follow northeast and northwest trends. Vertical, or steeply dipping faults, commonly bound small horst and graben structures. Many of the faults have histories of recurrent movement, with the latest

activity associated with regional crustal extension and development of the Rio Grande Rift. A major northeast-trending lineament, intersecting the Beidell volcanic center, 13 kilometers to the southwest, and the Klondike mining district, 16 kilometers to the northeast, is expressed in the study area by two flow-banded rhyolitic dikes.

Hydrothermal alteration extends over an area of approximately 13 square kilometers, centered about an area of small horst and graben structures. A high-silica alteration zone, comprised principally of jasperoid breccias, represents the most intense hydrothermal alteration in the study area. These rocks are irregularly enveloped by an "advanced argillic alteration zone" as defined by Hemley and Jones (1964). Non-brecciated, silicified quartz latites define a third alteration zone. Hydrolytic decomposition of silicate rocks has been interpreted as the most significant hydrothermal alteration process.

Hydrothermal alteration and trace metal geochemistry is not consistent with the porphyry ore deposit model (Lowell and Gilbert, 1970), and it is unlikely that a subsurface orebody of this type exists. Therefore, the most likely target for further exploration in the Tracy Canyon area are the jasperoid breccia pipes.

James W. Newman
Department of Earth Resources
Colorado State University
Fort Collins, Colorado 80521
Spring, 1976

ACKNOWLEDGEMENTS

The writer wishes to express special gratitude to Mr. W. A. Bowes of W. A. Bowes and Associates, Steamboat Springs, Colorado for providing the generous financial support and assistance. Special appreciation is extended to Dr. T. B. Thompson, thesis advisor, for assistance in the field and for his critical and constructive aid in completion of the manuscript. The writer is also deeply indepted to Dr. M. E. McCallum for his assistance in obtaining financial support and for serving on the thesis committee. Acknowledgement is gratefully accorded Dr. L. K. Burns for visiting the study area and for the useful discussions during completion of the manuscript. Appreciation is also extended to Dr. C. G. Warren of the Department of Chemistry for serving on the thesis committee.

Special thanks are extended to fellow graduate students, M. E. Donnelly, R. R. Loucks, and K. D. Black, for time spent in reviewing and discussion of the manuscript.

Very special appreciation is extended to my wife, René, for her invaluable assistance in the field and in the laboratory.

TABLE OF CONTENTS

Table of Contents, Continued

LIST OF TABLES

LIST OF FIGURES

List of Figures, Continued

LIST OF PLATES

INTRODUCTION

PURPOSE

The purpose of this study was to map in detail the geology and hydrothermal alteration of the Tracy Canyon area. Reconnaissance mapping and a soil geochemistry survey of the B. S. claim block (Pl. 1), acquired in 1969 and properly maintained by W. A. Bowes and Associates, indicated the possibility of a porphyry copper-molybdenum type deposit. The writer has attempted to evaluate the geology, alteration, and trace metal geochemistry of the Tracy Canyon area with respect to the well-developed exploration model for porphyry copper and molybdenum deposits (Lowell and Guilbert, 1970).

LOCATION OF AREA

The Tracy Canyon area is located in Saguache County, Colorado, approximately 13 kilometers southwest of the town of Saguache (Fig. 1). The study area encompasses about 30 square kilometers and lies in the eastern portion of the Laughlin Gulch 7.5 minute quadrangle and the western part of the Saguache 7.5 minute quadrangle.

Elevations range from 7,900 feet in the northeastern corner of the study area to 11,017 feet on Tracy Mountain at the southwestern edge of the area (Fig. 2). The topography is moderate, consisting of gentle rolling hills throughout much of the central and eastern portions

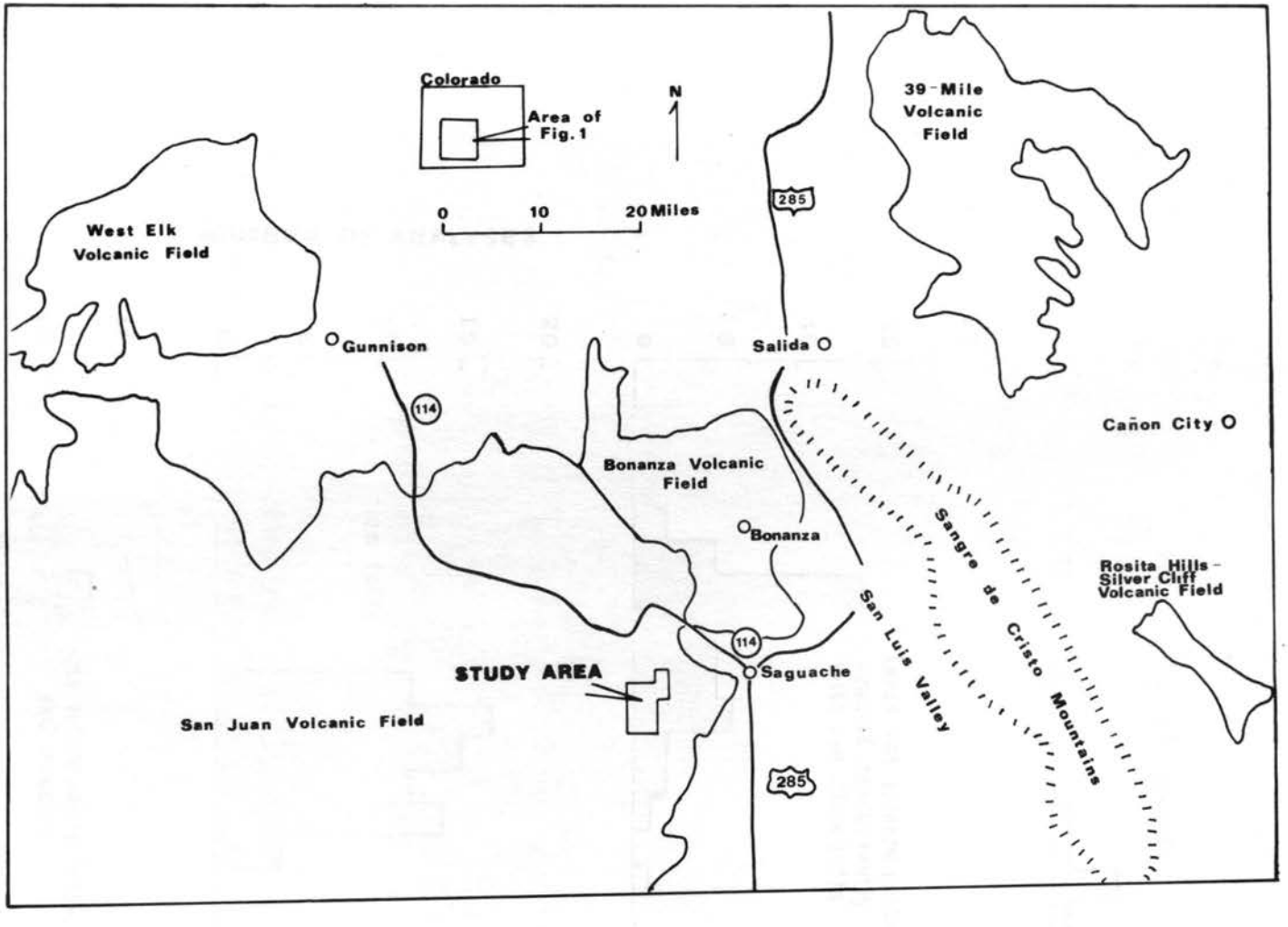

Figure 1. Index Map of Study Area.

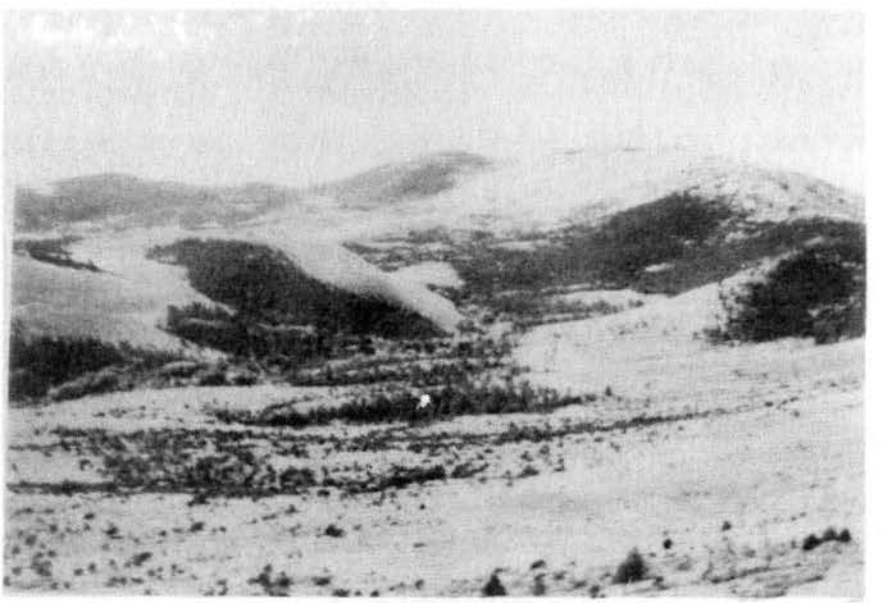

Figure 2. Photograph of North Tracy Canyon and Tracy Mountain from the east.

of the area and vertical cliffs surrounding the area on the north, south, and west.

At elevations under 10,000 feet much of the area is sparsely covered by shrub-like pinon and juniper with occasional stands of ponderosa pine. Aspen groves are common above 10,000 feet and along drainages. Other flora include a wide variety of wild flowers and several kinds of cacti. The Tracy Canyon area supports a number of different fauna, including blackbear, elk, mule deer, coyotes, porcupine, cottontail rabbit, and rattlesnakes.

The area may be reached from Saguache, Colorado by driving ten kilometers south on U.S. Highway 285, five kilometers west on a light-duty county road, and then approximately 13 kilometers west along an unimproved dirt road that parallels North Tracy Creek.

PREVIOUS STUDIES

Within the last century, the San Juan volcanic field has been extensively studied by a number of investigators. Whitman Cross began a regional study of the San Juan Mountains in 1895. He was later joined by Esper Larsen, and their efforts culminated with the publication of an exceptionally comprehensive report (Larsen and Cross, 1956) encompassing an area of 32,000 square kilometers. More recent reports dealing with the geology and lithology of the San Juan Mountains and radiometric ages of sparsely fossiliferous volcanics have greatly increased our understanding of the petrogenic

evolution of the San Juan volcanic field. Among the most notable of these papers are those by Steven and Epis (1968), Lipman (1968), Lipman et al. (1969), Lipman et al. (1970), and Lipman (1975). In spite of these studies, no detailed geologic work within the Tracy Canyon area has been published. Considerable attention has been given, however, to the rocks of the Bonanza volcanic center, approximately eight kilometers northeast of the study area, predominantly as graduate thesis research by students from the Colorado School of Mines. Petrologic relations 13 kilometers south of the study area are included in the Geologic Map of the Durango Quadrangle (Steven et al., 1974). The Durango quadrangle is remarkably detailed for a scale of 1:250,000.

An unpublished reconnaissance geologic map of the Tracy Canyon area was completed by W. A. Bowes and Associates of Steamboat Springs, Colorado in 1969.

METHODS OF INVESTIGATION

Field work was conducted during the summers of 1974 and 1975. An area of approximately eight square kilometers was mapped on a topographic base map enlarged from the U.S.G.S. Laughlin Gulch quadrange (1:24,000) to a scale of 1:6,000. To gain a better understanding of the geology of the surrounding area, reconnaissance mapping of an additional area of approximately 25 square kilometers was done on a base map enlarged from the U.S.G.S. Laughlin Gulch

and Saguache quadrangles (1:24,000) to a scale of 1:12,000. Black and white and infra-red high-altitude aerial photographs were also used as an aid in mapping.

W. A. Bowes and Associates graciously provided emission spectrographic analyses (Tom Hancock, analyst) of 280 rock chip samples collected in the field.

One hundred-fifty thin sections were examined by standard petrographic methods. Plagioclase compositions were determined utilizing the Michel-Lévy method as described by Kerr (1959, p. 257-260). Granodiorite and quartz monzonite slabs were selectively stained for K-feldspar according to the method described by Bailey and Stevens (1960, p. 1020-1025).

Lipman's (1975, p. 5) classification of volcanic rocks was employed, and SiO_2 contents were determined by the glass bead method as described by Kittleman (1963, p. 1405-1410).

Correlation coefficient matrices were determined by a standard S.P.S.S. computer program.

REGIONAL GEOLOGIC HISTORY

GENERAL STATEMENT

Volcanic rocks in the San Juan Mountains represent the largest erosional remnant of a once continuous volcanic field that extended over much of the southern Rocky Mountains in Oligocene and later time (Steven and Epis, 1968; Lipman et al., 1970). Extensive regional studies and the correlation of a large number of K-Ar age determinations indicate that the gross petrologic evolution throughout the San Juan volcanic field was relatively simple (Lipman et al., 1970). Volcanism began with intermediate lavas and breccias erupted from numerous local centers, followed closely in time by more silicic ash-flow tuffs and related lavas. Late-stage volcanism in the San Juan volcanic field is characterized by a bimodal association of basalt and high-silica alkali rhyolite.

EARLY INTERMEDIATE LAVAS AND BRECCIAS

The first evolutionary stage of the San Juan field was characterized by tremendous volumes of intermediate lavas and breccias--mainly alkali andesite, rhyodacite, and mafic quartz latite--erupted from numerous local volcanic centers upon a tectonically stable, eroded terrane. K-Ar age dates indicate that the early intermediate lavas and breccias of the Conejos Formation in the eastern and

southeastern San Juan Mountains were erupted during a relatively short interval 35 - 30 m.y. ago (Lipman et al., 1970).

ASH-FLOW TUFFS

As the Oligocene epoch came to a close, the nature of the volcanic activity changed to violent ash-flow eruptions of quartz latite and low-silica rhyolite. More than 16 major ash-flow sheets have been recognized, with at least 14 large cauldron complexes identified as source areas for these rocks (Lipman, 1975). The original areal extent of the ash-flow tuffs was similar to that of the early intermediate lavas. The pyroclastic rocks, however, are about half as voluminous as the older volcanics. K-Ar dating indicates that the ash-flow tuffs were erupted during the interval 30 - 26 m.y. ago (Lipman et al., 1970).

Subordinate volumes of intermediate and silicic lava flows and breccias intertongue with and overlie the ash-flow sequence. Many are petrographically and chemically similar to the ash-flow tuffs and are probably genetically related. Others may represent waning phases of early intermediate volcanism.

A few shallow laccoliths and stocks intrude the ash-flow sequence. They are most prevalent in the northern, western, and southeastern parts of the San Juan field (Lipman et al., 1969). These small intrusives are mostly monzonites and granodiorites, distinctly less silicic than the ash-flow tuffs and compositionally equivalent to the

early intermediate assemblage. They probably represent minor intermittent renewals of the Oligocene activity.

LATE BIMODAL ASSOCIATION

Late volcanic activity in the San Juan Mountains is characterized by a bimodal association of alkali olivine basalt to basaltic andesite and silicic alkali rhyolites. The basaltic flows occur as a widespread thin veneer, far less voluminous than the Oligocene intermediate flows and ash-flow tuffs. The rhyolite is a relatively minor phase that occurs predominantly as small volcanic necks and as local welded ash-flow tuffs. Mixed lava complexes, where rhyolitic and basaltic lavas have intermingled, are common. Hybridized basalts often contain rounded xenocrysts of quartz and alkali feldspar. Larsen and Cross (1956) mapped the basalts and rhyolites as the Hinsdale Formation. Hinsdale volcanism extended from 23 to about 5 m.y. ago (Lipman et al., 1970).

The final bimodal episode in the evolution of the San Juan volcanic field was accompanied by regional crustal extension and the development of the Rio Grande Valley block-fault system of southern Colorado and New Mexico. Inception of the final episode of bimodal volcanism and associated regional extension approximately corresponds in time with the destruction of the arc-trench system, as the North American Plate overrode the East Pacific Rise (Christiansen and Lipman, 1972; Lipman et al., 1970).

The Tertiary volcanic evolution of the San Juan Mountains is summarized in Fig. 3 and 4.

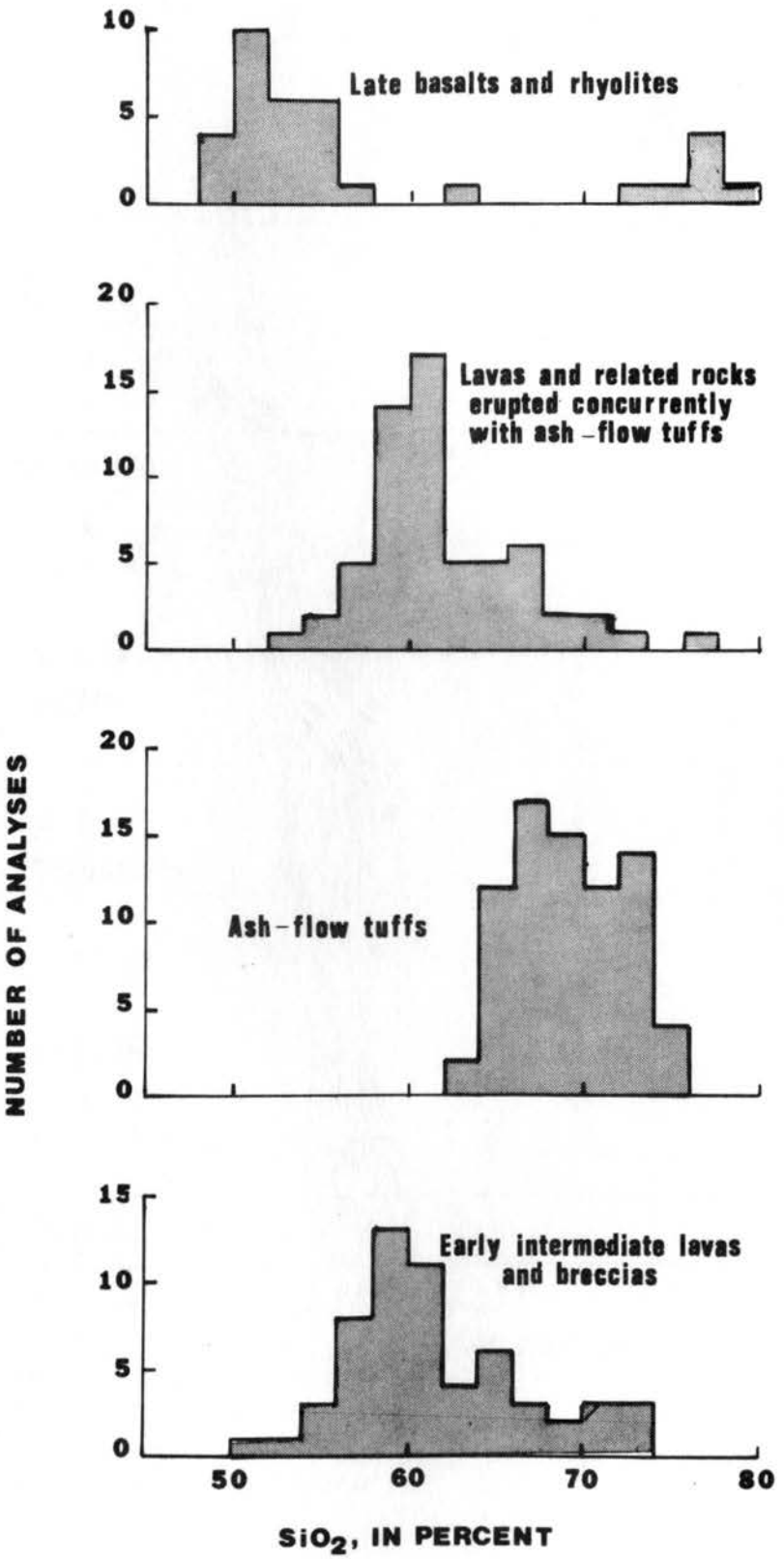

Figure 3. Histograms of SiO_2 contents for major divisions of San Juan volcanic rocks (from Lipman et al., 1970, Fig. 2).

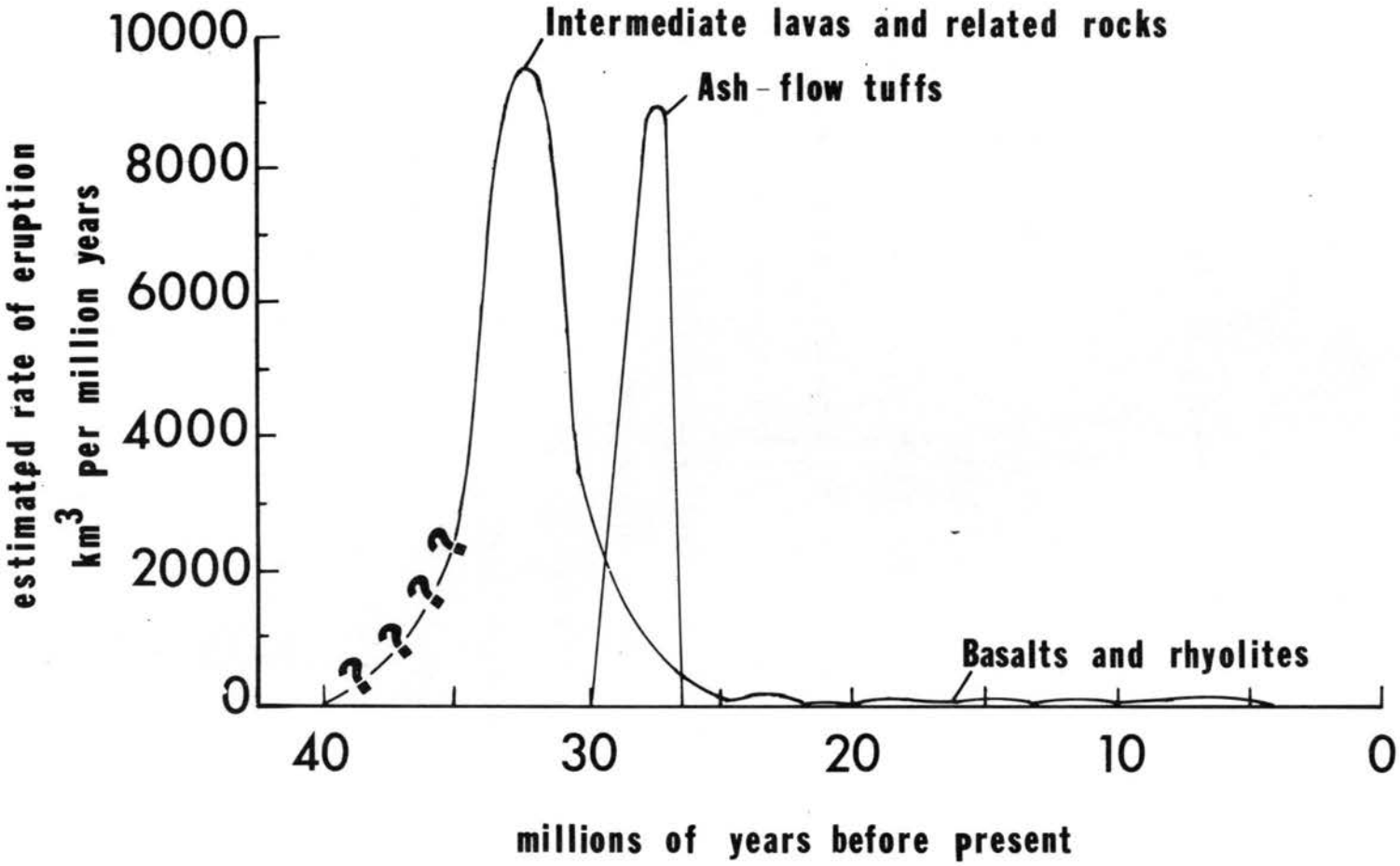

Figure 4. Relation between volume and time for the major petrologic divisions of the San Juan field (from Christiansen and Lipman, 1972, Fig. 4).

GEOLOGY OF THE TRACY CANYON AREA

PRE-TERTIARY ROCKS

No rocks older than Oligocene have been identified in the thesis area. A few low hills and small knobs of Precambrian rocks crop out about six kilometers north of the thesis area (James, 1971, p. 35) where they occur as small windows in Tertiary volcanics. Outcrops of Paleozoic rocks are largely limited to the western San Juan Mountains. A few small exposures of Paleozoic sediments have been reported in the drainage area of Kerber Creek (Larsen and Cross, 1956, p. 41), several kilometers northeast of the study area. Mesozoic sediments are best exposed in the western and southwestern portions of the San Juans. The complete Mesozoic section is well exposed near Durango, Colorado in the southwestern San Juan region (Larsen and Cross, 1956, p. 48).

TERTIARY VOLCANICS

Volcanic flows and flow breccias of the early intermediate assemblage are well represented in the study area and include andesites, rhyodacites, and quartz latites. These rocks, members of the Conejos Formation, are partially capped by olivine basaltic andesites of the Hinsdale Formation. No pyroclastics crop out in the study area.

Because most of the rocks in the study area are glassy or at least partly aphanitic, rock names must be based on chemical composition. The following scheme, employed by Lipman (1975, p. 5), is utilized in this study.

	Percent SiO_2
Basalt	less than 52
Andesite	52-60
Rhyodacite	60-65
Quartz Latite	65-70
Rhyolite	greater than 70

Silica percentages were determined utilizing the refractive index-silica technique (Kittleman, 1963). Figure 5 plots the index of refraction for volcanics of Tracy Canyon area on the regression line developed by Kittleman (1963, p. 1408). Table 1 shows the SiO_2 contents for these rocks as determined by the refractive indices of glass beads.

This method has been employed in previous Colorado State University theses with apparent success (Beverly, 1969, p. 54; Samuelson, 1971, p. 38). However, as a precaution against possible contamination effects, several samples were refused and the R.I. redetermined. In each case, the difference in the index of refraction was no greater than 0.002. The regression curve was tested by fusing a standard of known chemical composition. The SiO_2 content, determined by the index of refraction of the glass bead, was within the 2 percent standard deviation given by Kittleman for the regression curve.

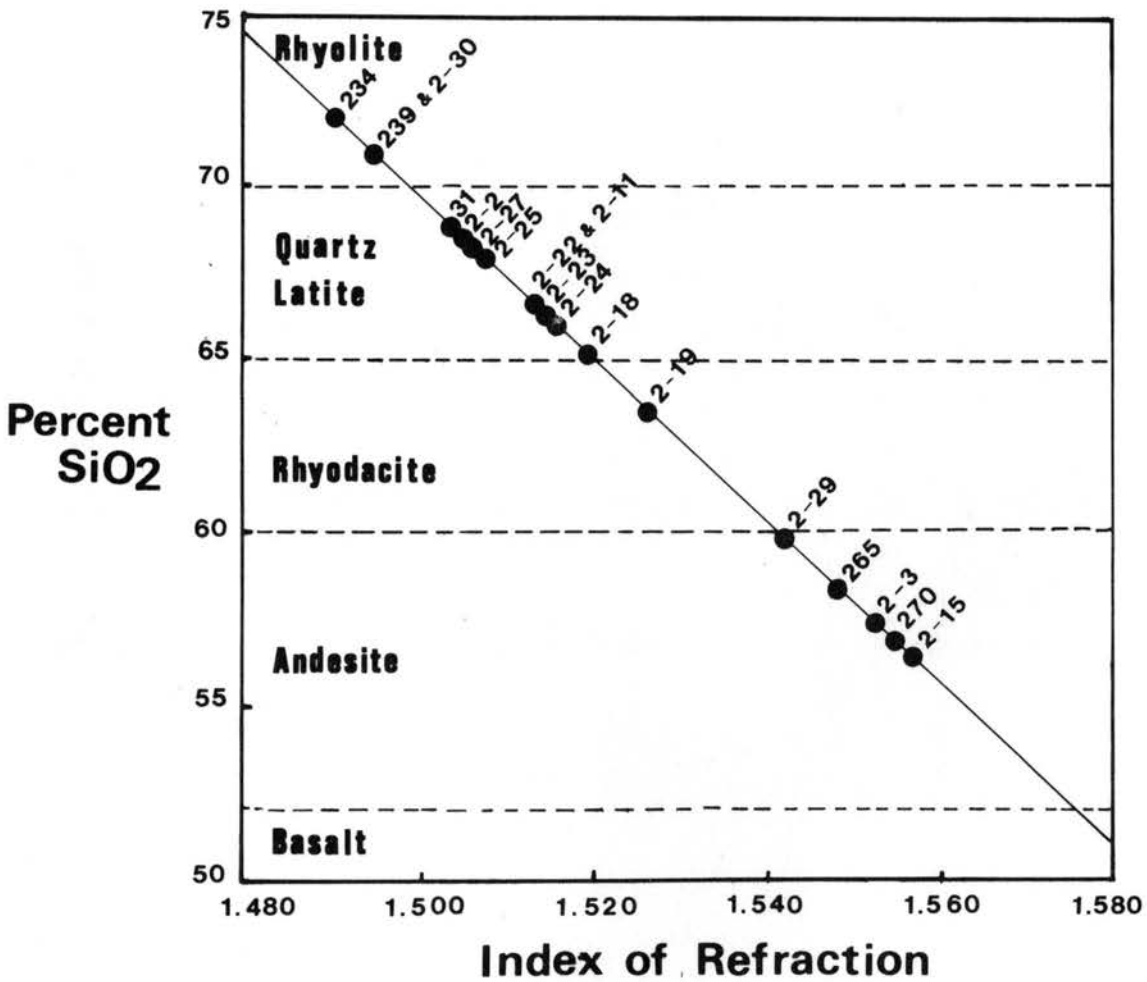

Figure 5. Index of refraction for volcanics of Tracy Canyon area are plotted on the regression line developed by Kittleman (1963, p. 1408). Rock names are based on the classification scheme employed by Lipman (1975, p. 5).

Table 1. Estimated SiO_2 percentages of Tracy Canyon area volcanics. Percentages are determined from regression line calculated by Kittleman (1963, p. 1408). Rocks are named according to Lipman's classification (1975, p. 5).

Sample	Index of Refraction	Percent SiO_2
RHYOLITE, Tr_{hy}		
BS-234	1.496	72.0
BS-239	1.501	70.9
BS-2-30	1.501	70.9
QUARTZ LATITE, $Tqlp_1$		
BS-31	1.510	68.8
BS-2-25	1.513	68.0
BS-2-27	1.512	68.3
BS-2-2	1.511	68.5
QUARTZ LATITE, $Tqlp_2$		
BS-2-24	1.525	65.2
BS-2-23	1.520	66.4
BS-2-22	1.519	66.6
BS-2-11	1.519	66.6
RHYODACITE, Trdp		
BS-2-18	1.533	63.3
BS-2-19	1.520	66.4
ANDESITE, Tap		
BS-265	1.555	58.2
BS-2-29	1.549	59.6
BS-2-3	1.558	57.5
BASALTIC ANDESITE, Tba		
BS-2-15	1.562	56.5
BS-270	1.560	57.0

Conejos Formation

Early intermediate lavas belonging to the Conejos Formation have been subdivided into four discrete flow units: early porphyritic quartz latites, mafic porphyritic quartz latites, porphyritic andesites, and porphyritic rhyodacites.

Porphyritic quartz latite ($Tqlp_1$) -- The oldest rocks exposed in the thesis area are purple to brown, porphyritic biotite-hornblende quartz latite flows and flow breccias. Small outcrops are scattered throughout the area, but the best exposures occur in the northeast and southwest portions of the study area (Pl. 1). To the southwest, vertical exposures are greater than 150 meters, but the unit was probably originally much thicker. Outcrops are generally tabular exhibiting vertical or steeply-dipping joints.

Megascopically, the rocks are purple to reddish-brown. Phenocrysts of plagioclase, biotite, and hornblende are visible and commonly demonstrate good flow alignment. The flow breccias consist of angular lithic fragments in a matrix of the same material.

Microscopically, the quartz latites exhibit a porphyritic to glomeroporphyritic texture with 10-15 percent of the rock consisting of subhedral to euhedral phenocrysts of plagioclase, biotite, oxyhornblende, and minor magnetite (Table 2).

Subhedral andesine (An_{40}) laths are the dominant phenocryst phase. They commonly are normally zoned and are up to 2.5 mm

Table 2. Modal analyses (volume percent) for early porphyritic quartz latite.

	Sample				
	BS-31	BS-216	BS-221	BS-2-8	BS-2-1
Groundmass	84.5	84.7	87.5	92.3	92.3
Plagioclase	10.2 An_{40}	10.5 An_{44}	8.1 An_{44}	5.7 An_{38}	6.6 An_{35}
Biotite	4.2	3.0	1.9	0.5	0.7
Hornblende	0.3	1.0	--	0.8	--
Magnetite	0.8	0.8	2.5	0.8	0.3
Apatite	tr	tr	tr	tr	tr
Hematite	tr	--	tr	tr	tr

long. The plagioclase phenocrysts may be found in glomeroporphyritic aggregates with other phenocrysts but usually occur as individual subparallel laths.

Reddish-brown oxidized biotite laths are the next most abundant phenocrysts (Fig. 6). They commonly have been replaced by magnetite along crystal borders and cleavage traces. They are up to 2.5 mm long and exhibit excellent flow alignment.

Reddish-brown oxyhornblendes are less abundant than biotite. They occur as euhedral to subhedral crystals, up to 2 mm in their greatest dimension (Fig. 7), and have been largely replaced by magnetite.

The pilotaxitic groundmass consists of subparallel microlites of plagioclase with interstices occupied by brown volcanic glass, flakes of biotite, and granular iron ore. Accessory minerals include apatite and hematite.

Porphyritic mafic quartz latite ($Tqlp_2$) -- This unit is a mafic quartz latite that blankets the earlier quartz latites in the north and northcentral parts of the thesis area (Pl. 1). It is relatively flat lying, and best exposures occur in the northern portion of the study area where it forms cliffs with more than 120 meters of vertical relief. The unit pinches out to the south, indicating the source area was probably north or northeast of the study area. Contacts at the base of the unit are fairly regular, and the mafic quartz latite was

Figure 6. Porphyritic quartz latite ($Tqlp_1$) Plane light. Biotite (B) and plagioclase (P) phenocrysts display subparallel flow alignment with pilotaxitic groundmass.

Figure 7. Porphyritic quartz latite ($Tqlp_1$) Plane light. Euhedral hornblende (H) and plagioclase (P) phenocrysts display good flow alignment with pilotaxitic groundmass.

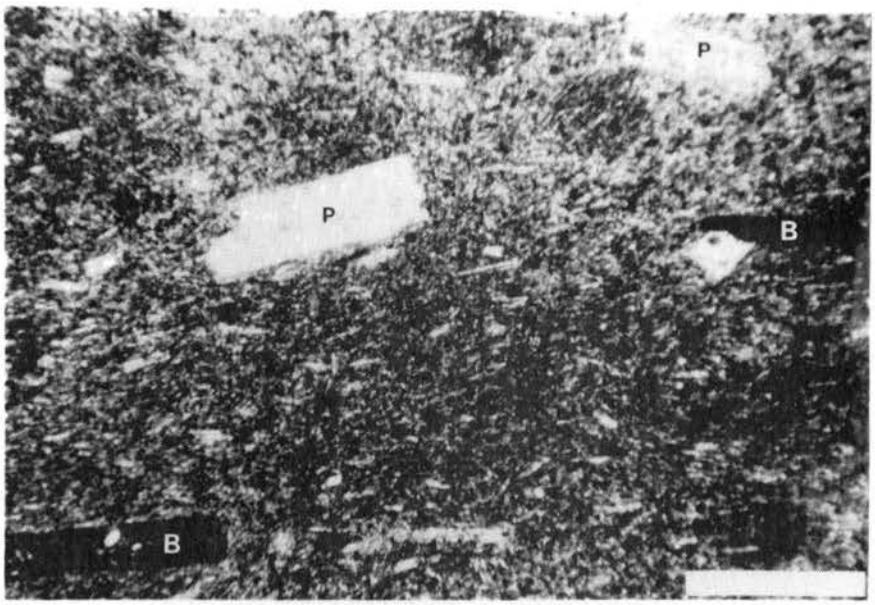
P
P
B
B
1 mm

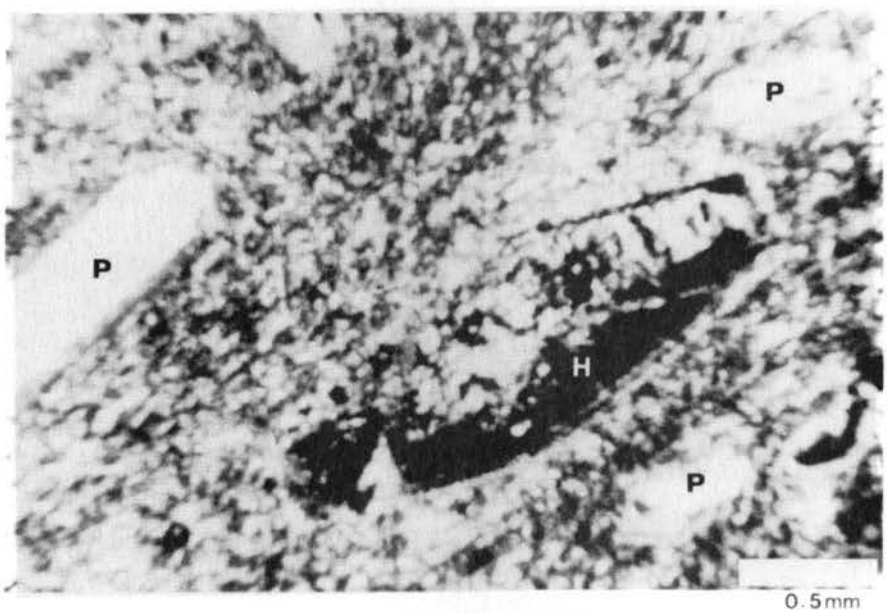
P
P
H
P
0.5mm

probably erupted shortly after deposition of the early quartz latitic unit.

Megascopically, the unit consists of brown to gray, porphyritic flows and breccias. The breccias are autobreccias which appear to be restricted to the base of the unit. Phenocrysts include plagioclase, biotite, hornblende, and pyroxene. Flow structures are not as well developed as in the older quartz latites.

Microscopically, the younger quartz latites exhibit glomeroporphyritic to cumuloporphyritic texture. Phenocrysts make up 30-40 percent of the rock. Modal analyses of five mafic quartz latite samples are included in Table 3. Subhedral to euhedral laths of calcic andesine to sodic labradorite (An_{44-52}), up to 2.5 mm long, are the dominant phenocryst. They commonly occur in aggregates with other phenocrysts, and less commonly, in aggregates with phenocrysts of biotite and pyroxene. The plagioclase phenocrysts are commonly normally zoned and possess numerous irregular inclusions of brown volcanic glass. Subhedral, reddish-brown, biotite laths are the next most abundant phenocryst phase. They are generally less than 1 mm in length and demonstrate poor to fair flow alignment. The biotite phenocrysts are often largely or completely replaced by magnetite. Euhedral, unaltered augite phenocrysts make up 2-3 percent of the rock. In addition to occurring as a replacement product, equant grains of primary magnetite are always present in amounts of 2-3

Table 3. Modal analyses (volume percent) for mafic porphyritic quartz latite.

	Sample				
	BS-2-10	BS-2-12	BS-2-9	BS-2-24	BS-2-11
Groundmass	67.8	66.5	59.7	70.2	67.9
Plagioclase	25.6 An_{48}	25.3 An_{52}	28.4 An_{49}	21.8 An_{44}	24.3 An_{48}
Biotite	1.9	3.8	5.6	3.1	2.8
Augite	0.9	1.2	2.2	1.6	1.5
Magnetite	2.5	2.3	3.1	3.2	3.1
Hypersthene	1.4	1.0	--	--	--
Hornblende	--	--	1.0	--	--
Quartz	--	--	--	--	0.4
Talc	--	--	--	--	tr
Hematite	--	--	tr	tr	tr
Apatite	tr	tr	tr	tr	tr

percent. Reddish-brown oxyhornblende, hypersthene, and quartz may be present in small amounts.

The orthophyric groundmass consists of stumpy, rectangular plagioclase grains, acicular crystals of biotite, and brown, partially devitrified, volcanic glass. Accessory minerals include apatite and hematite.

Porphyritic andesite (Tap and Tia) -- Dense, dark gray exposures of porphyritic andesite crop out throughout the thesis area. Best exposures occur in the east-northeast portion of the study area where continuous andesitic flows overlie quartz latitic rocks (Pl. 1). Throughout the remainder of the area the andesites occur as small discontinuous dikes and as lenses and narrow elongate bodies. These rocks probably represent vestiges of a thin andesite veneer that once covered much of the area. In the southern portion of the study area, andesitic lavas have been truncated by younger rhyodacitic flows. Cross-cutting relations between the andesitic dike and flow rocks were not observed and because of similar composition and petrology, they have been included together. It is possible that the andesitic flow and dike rocks in the study area represent multiple episodes of andesite activity.

Megascopically, the andesitic rocks are dark gray to black. They exhibit porphyritic textures with phenocrysts of plagioclase and pyroxene being most abundant. Outcrops are blocky and commonly exhibit vertical or steeply-dipping joints.

Microscopically, the andesites exhibit porphyritic to glomeroporphyritic textures. Subhedral laths of plagioclase (An_{45-54}) up to 3 mm in their greatest dimension are the dominant phenocryst. They commonly are normally zoned and occasionally exhibit oscillatory zoning. The feldspar phenocrysts sometimes show a crude flow alignment, but most commonly occur as randomly oriented grains, often in glomeroporphyritic aggregates with clino- and orthopyroxenes, biotite, and magnetite. Euhedral to subhedral augites are the next most abundant phenocryst. They comprise up to 5 percent of the rock and often exhibit polysynthetic twinning. Some augite grains rim irregular grains of earlier-crystallized hypersthene (Fig. 8). Stongly pleochroic phenocrysts of hypersthene, or its deuteric alteration products, are found in subordinant amounts in most of the andesitic rocks. Reddish-brown biotite makes up 2-3 percent of the rock and occurs as subhedral laths less than 1 mm long and as irregular, anhedral flakes, commonly partially enclosing small grains of magnetite.

The groundmass ranges from pilotaxitic, in which the feldspar microlites are aligned by flowage, to vitrophyric in texture. One sample, BS-2-4, exhibits excellent perlitic structure with concentric cracks caused by rapid cooling after extrusion (Fig. 9). Modal analyses of seven andesite samples are presented in Table 4.

Many of the andesites have undergone slight to moderate propylitic alteration. The biotite phenocrysts commonly are replaced by

Figure 8. Photomicrograph of porphyritic andesite (Tap) (polarized light). Glomeroporphyritic aggregate with clinopyroxene (A), orthopyroxene (H), and magnetite (M) in a vitrophyric groundmass. Note the clinopyroxene enclosing the orthopyroxene grain.

Figure 9. Photomicrograph of porphyritic andesite (Tap) (polarized light). Phenocrysts of plagioclase (P) and augite (A) in a black vitrophyric groundmass with perlitic texture.

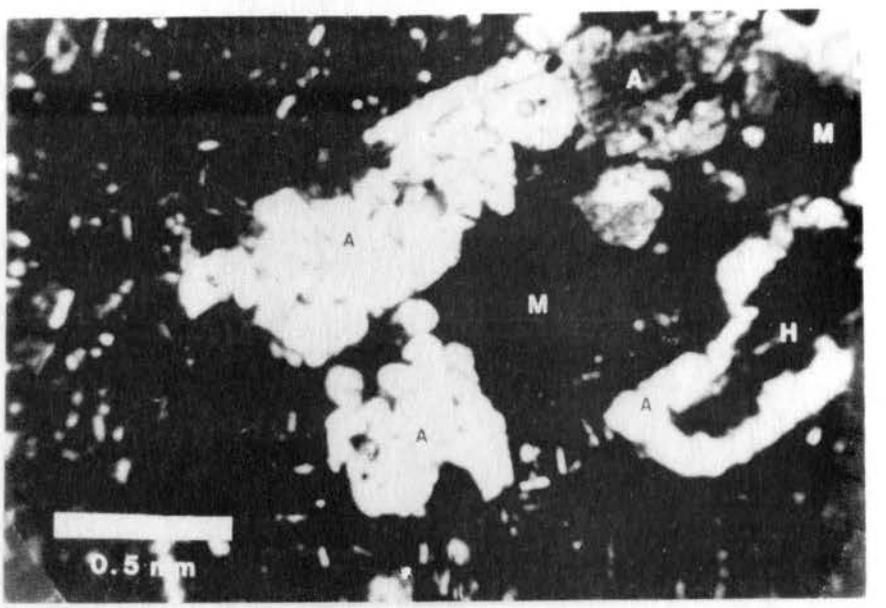
A
M
A
M
H
A
A
0.5 mm

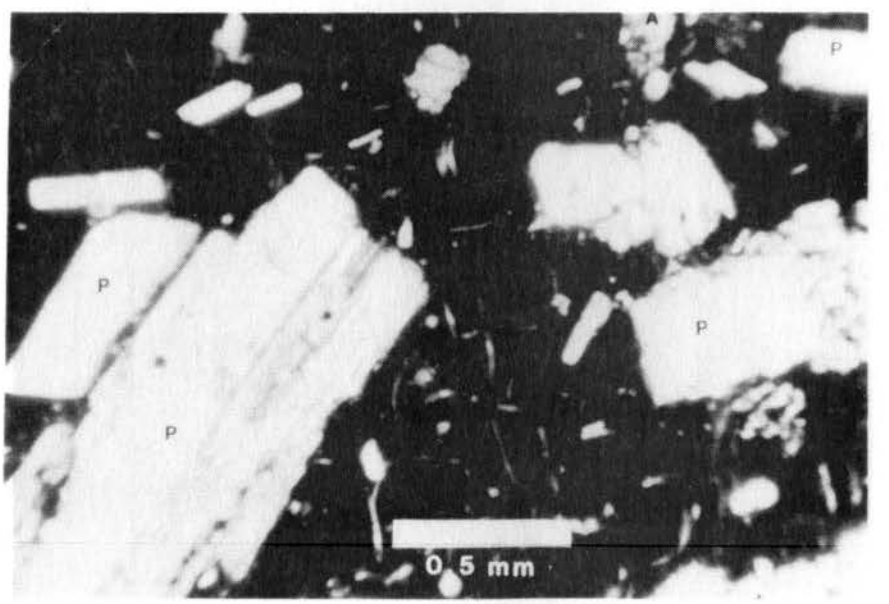
A
P
P
P
P
0.5 mm

Table 4. Modal analyses (volume percent) for extrusive and intrusive Tertiary andesites.

	Sample						
	BS-2-5	BS-2-4	BS-236	BS-224	BS-289	BS-185	BS-148
Groundmass	71.4	68.5	84.9	61.6	80.4	82.2	79.1
Plagioclase	20.6 An_{45}	19.8 An_{44}	8.9 An_{54}	26.5 An_{50}	11.6 An_{52}	10.3 An_{54}	13.9 An_{45}
Augite	3.0	4.6	1.1	5.1	5.5	3.3	1.7
Hypersthene	1.6	2.7	3.2	--	--	--	--
Biotite	2.3	2.4	0.4	--	--	--	2.4
Magnetite	1.2	2.0	1.2	2.8	2.3	1.9	2.8
Bastite	--	--	--	1.9	0.3	2.3	--
Iddingsite	--	--	--	--	--	tr	--
Calcite	--	--	0.4	--	tr	--	--
Apatite	tr	tr	tr	tr	--	tr	--

secondary chlorite and magnetite, and the feldspars and pyroxenes have commonly been altered to calcite and epidote. The distribution of propylitic alteration shows no relation to the hydrothermal alteration in the study area and is entirely a deuteric process.

Porphyritic rhyodacite (Trdp) -- The youngest rocks exposed in the study area, belonging to the early intermediate Conejos Formation, are light gray hornblende rhyodacite flows. Exposures are limited to the extreme southern portion of the mapped area (Pl. 1), and the unit thickens to the south, indicating the direction of the probable source area. Its overall areal extent was not determined, but it was probably quite extensive. Outcrops are tabular to angular and have vertical or steeply-dipping joints.

Megascopically, the rocks are light gray and display porphyritic textures with tabular phenocrysts of plagioclase and hornblende. Flow structures are moderately well developed.

Microscopically, the rhyodacitic rocks exhibit porphyritic textures with a cryptocrystalline to pilotaxitic groundmass. The phenocrysts comprise between 25 and 50 percent of the rock and show fair to good flow alignment. Subhedral laths of andesine (An_{41-44}) are the dominant phenocryst. They make up between 15 and 20 percent of the rock, are commonly normally zoned, and are up to 3 mm long. Subhedral to euhedral, reddish-brown oxyhornblende phenocrysts comprise between 5 and 10 percent of the rock. They are up to 2 mm in their greatest dimension and are largely replaced by magnetite.

Reddish-brown biotite laths make up about 5 percent of the rock and have been replaced by magnetite along crystal borders and along cleavage planes. The remainder of the phenocrysts include euhedral, colorless augite; anhedral quartz; and subhedral, equant grains of magnetite. Modal analyses of two rhyodacite samples are presented in Table 5.

Table 5. Modal analyses (volume percent) for rhyodacite prophyry.

	Sample	
	BS-2-18	BS-2-17
Groundmass	55.0	73.0
Plagioclase	21.5 An_{44}	16.5 An_{41}
Hornblende	9.0	4.4
Augite	4.2	1.4
Biotite	3.5	3.0
Magnetite	3.9	1.7
Quartz	2.8	--

Hinsdale Formation

Based on composition and stratigraphic position, the basaltic andesite flows capping Tracy Mountain on the western margin of the thesis area and a down-dropped structural graben in the central portion of the area have been mapped as part of the Hinsdale Formation (Pl. 1).

Basaltic andesites (Tba) - The youngest flows exposed in the study area are light gray, vesicular basaltic andesites. They occur on the extreme western margin of the thesis area and on a structurally down-dropped block in the central part of the area, where they overlie quartz latites of the Conejos Formation. Best exposures occur near the summit of Tracy Mountain. The unit appears to be relatively flat-lying and shows no evidence of hydrothermal alteration. The areal extent and thickness of the unit were not determined, as much of it lies outside the base map area.

Megascopically, the rocks are light gray, vesicular, and exhibit fine-grained porphyritic textures. Field identification is facilitated by the abundance of iddingsite, the conspicuous brownish-red alteration product of olivine. Phenocrysts of plagioclase and augite are also visible.

Microscopically, the basaltic andesite is a gray, vesicular, porphyritic to glomeroporphyritic rock. Subhedral labradorite (An_{50-55}) laths are the most abundant phenocryst and occur up to 3 mm long.

The feldspar phenocrysts make up 20-30 percent of the rock and may occur in glomeroporphyritic aggregates with clinopyroxene and olivine or as individual laths, commonly exhibiting a crude flow alignment. Subhedral to euhedral pale brown augite phenocrysts are the next most abundant. They are up to 1 mm in diameter and make up 10-15 percent of the rock. Subhedral olivine and its alteration products, magnetite and iddingsite, comprise 5-10 percent of the rock. Most of the olivine crystal have been almost entirely replaced by secondary products. A few of the phenocrysts have escaped the intense alteration, however, and are altered only along the outer iron-rich rims and along irregular fractures. The vesicular, intergranular groundmass makes up 50-65 percent of the rock and consists of granules of clinopyroxene and iron ore occupying angular interstices between plagioclase microlites. Modal analyses of four olivine basaltic andesites are presented in Table 6.

TERTIARY INTRUSIVES

Intrusives in the study area represent all of the major episodes of San Juan volcanism. Small, discontinuous andesitic dikes may represent the oldest intrusive rocks exposed in the area. They are similar in chemistry and petrology to the andesite flows of the Conejos Formation, and are probably equivalent in age. Some of the andesites have not been effected by hydrothermal alteration, and probably represent a late andesitic event. A small granodioritic

Table 6. Modal analyses (volume percent) for basaltic andesite.

	Sample			
	BS-2-13	BS-2-14	BS-2-16	BS-2-15
Groundmass	50.9	53.2	64.2	68.3
Plagioclase	29.9 An_{54}	28.5 An_{55}	19.1 An_{52}	20.4 An_{54}
Augite	12.5	14.4	8.7	6.8
Hypersthene	0.8	--	--	--
Olivine	--	--	1.3	--
Magnetite	2.8	1.2	6.1	1.5
Iddingsite	3.1	2.6	0.7	3.0
Apatite	tr	--	--	--

stock intrudes andesitic and rhyodacitic lavas of the early intermediate assemblage. Rocks of the granodiorite stock, and related intrusives, are probably representatives of the late Oligocene activity. The bimodal episode of volcanism is characterized in the study area by small hybridized dikes and two, flow-banded, high-silica rhyolitic dikes.

Late Oligocene Stock

Small laccoliths and stocks, mostly monzonites and granodiorites, are exposed throughout the San Juan volcanic field. They commonly intrude or intertongue with ash-flow tuffs and are believed to represent minor intermittent renewals of the early intermediate Oligocene magmatism (Lipman et al., 1969).

Granodiorite stock (Tgrd) -- A small, mafic granodioritic stock crops out in the south-central part of the study area (Pl. 1). The stock is roughly rectangular in plan view with the longer axis oriented to the northeast. The surface dimensions are approximately 550 by 1,000 meters. The body is bounded on its eastern and western borders by northwest-trending faults. The stock intrudes both andesitic and rhyodacitic lavas of the early intermediate association. The field relations, together with the chemical and compositional character of the intrusive, support the interpretation that the granodiorite stock represents an episode of late Oligocene resurgence of the early intermediate volcanic activity. The northern border of the intrusive

is in sharp contact with early intermediate andesitic lavas. Two small exploration pits along the contact expose iron-oxide stained, brecciated, and altered rocks. The sharp contact between the stock and the volcanics probably provided an avenue for later hydrothermal fluids.

In hand specimen, the granodiorite is light gray to olive-green, medium-grained, and equigranular. Field identification is facilitated by the tendency of the unit to weather into bouldery outcrops.

Microscopically, the granodiorite is a gray, medium-grained, hypidiomorphic granular rock. Between 40 and 50 percent of the rock consists of normally zoned, subhedral andesine (An_{42}) grains up to 3 mm in their greatest dimension. Anhedral orthoclase makes up 15-20 percent of the rock. It occurs as isolated grains, up to 2 mm in its greatest dimension, and as granophyric intergrowths with acicular webs of quartz. Quartz makes up about 10 percent of the rock and is found as intergrowths with orthoclase and as anhedral grains in interstices between the other minerals. Subhedral to euhedral augite crystals make up 5-10 percent of the rock. They are commonly corroded and partly altered. Aggregates of chlorite and magnetite occur in clusters and constitute about 15 percent of the rock. They are probably the deuteric alteration products of magmatic hornblende. Reddish-brown, anhedral biotite flakes make up about 5 percent of the rock. Apatite is a common accessory mineral. Table 7 presents modal analyses for two of the mafic granodiorite samples.

Table 7. Modal analyses (volume percent) for mafic granodiorite.

	Sample	
	BS-2-21	BS-2-20
Plagioclase	43.0 An_{46}	47.5 An_{38}
Orthoclase	16.6	18.5
Quartz	6.9	10.6
Biotite	5.4	4.1
Augite	12.6	4.3
Magnetite	6.9	3.9
Chlorite	9.0	11.1
Apatite	tr	tr

Mafic dike (Tgrdi) -- Hybridized rocks exhibiting a peculiar texture crop out in a dike near the northern edge of the granodiorite stock. They occur along a northwest-trending fault where they intrude Tertiary andesites of the Conejos Formation. The dike is approximately 15 meters wide and 60 meters long.

Megascopically, the rocks are light gray to olive-green and have a porphyritic appearance with black, rounded, "anhedral crystals" up to 5 mm in diameter.

Microscopically, the dike rocks are medium-grained and holocrystalline with an allotriomorphic granular texture. The mafic

minerals augite, biotite, hornblende, olivine, and magetite comprise approximately 50 percent of the rock; anhedral plagioclase (An_{42}) and minor orthoclase comprise the remainder of the rock. Reddish-brown biotite and hornblende crystals and colorless augite grains occur as randomly dispersed, anhedral, rounded blebs and as mafic clots, along with irregular cummulate aggregates of olivine and anhedral grains of magnetite. Anhedral grains of andesine up to 3 mm in length are highly corroded and irregular in shape. Apatite is a common accessory mineral.

Similarities in texture, mineralogy, and location between these rocks and rocks from the mafic granodiorite stock suggest that they may have been co-magmatic. The dike rocks are probably the product of a younger differentiated silicate melt that incorporated earlier-crystallized mafic xenoliths. The texture and mineralogy of this unit probably reflects incomplete attainment of chemical equilibrium between the two phases.

Porphyritic quartz monzonite (Tqmp) -- Associated with the granodiorite stock are numerous small pods and discontinous outcroppings of leucocratic quartz monzonite. Small inclusions of quartz monzonitic rocks are also found in the mafic dike and in andesitic rocks near the northern border of the stock (Pl. 1). These rocks may represent satellitic offshoots from the granodiorite. Still further magmatic differentiation may have yielded the hydrothermal solutions that invaded the volcanic rocks in the Tracy Canyon area.

Macroscopically, the rocks are light gray to tan and display porphyritic to coarse-grained, almost pegmatitic, textures. Phenocrysts consist of plagioclase, orthoclase, and quartz. The dearth of ferromagnesian minerals is conspicuous. The feldspar phenocrysts are often argillized, and unweathered exposures are rare.

Microscopically, the quartz monzonitic rocks display porphyritic textures and felsophyric groundmasses. Plagioclase phenocrysts make up approximately 40 percent of the rock and occur as anhedral grains up to 6 mm in their greatest dimension. They are commonly argillized, and the albite twinning has been largely obliterated. Quartz phenocrysts make up about 20 percent of the rock and occur as anhedral grains up to 5 mm in their greatest dimension. They exhibit interlocking and sutured grain boundaries and commonly possess undulatory extinction. Orthoclase occurs as irregular phenocrysts with large quartz and plagioclase grains. Sodium-cobaltnitrite staining for K-feldspar indicates it is limited primarily to the felsophyric groundmass. Biotite phenocrysts make up less than 5 percent of the rock. The grains are generally highly corroded and have been replaced by magnetite and chlorite. The mosaic-like felsophyric groundmass has been argillized and is a heterogeneous aggregate, exhibiting various intergrowth and interlocking textures.

The coarse grain size and the shattered and strained appearance of these rocks in thin section suggests that they crystallized at depth and were subsequently transported to the surface by the hypabyssal

intrusives. They may be much older than the rocks they are included in, and not magmatically related.

Hybridized Intrusives of the Late Bimodal Association

Mixed lava complexes, where rhyolitic and basaltic lavas have intermingled, are characteristic of late volcanic activity in the San Juan Mountains. Four small, hybridized dikes of this nature crop out in the Tracy Canyon area.

Hybridized basaltic andesite (Tb_{hy}) -- Three small, hybridized basaltic andesite dikes crop out in the north and northwestern portions of the study area (Pl. 1). They intrude unaltered mafic quartz latites and highly-altered older quartz latites. The dike rocks are unaltered and are probably equivalent in age to the Hinsdale Formation of Larsen and Cross (1956). They appear in outcrop as angular, unweathered elongate bodies.

Megascopically, the hybridized dike rocks are dark-gray to black and are porphyritic, plagioclase being the dominant phenocryst.

In thin section, the rocks exhibit a holocrystalline, cumuloporphyritic to glomeroporphyritic texture. The felsophyric to orthophyric groundmass generally makes up 60-70 percent of the rock. Plagioclase phenocrysts, up to 5 mm in length, make up 20-25 percent of the rock. They are An_{40-48} in composition, normally zoned, and possess numerous resorption pits. Reddish-brown, subhedral to euhedral augite phenocrysts are the next most abundant (Fig. 10); the remainder of

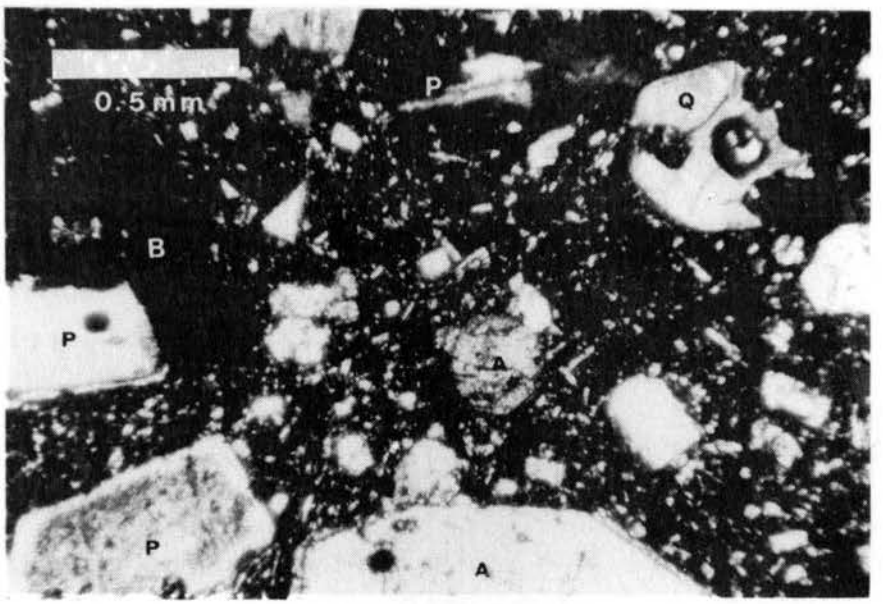

Figure 10. Photomicrograph of porphyritic hybridized basaltic andesite (plane light). Phenocrysts of plagioclase (P), augite (A), biotite (B), and xenocryst of quartz (Q).

the phenocrysts include minor amounts of subhedral hypersthene, reddish-brown biotite, oxyhornblende, bastite pseudomorphs after olivine (Fig. 11), and magnetite. Corrosively rounded sanidine grains in disequilibrium with the other phenocrysts make up 1-2 percent of the rock, and rounded, embayed quartz xenocrysts make up another percent. Apatite is an abundant accessory mineral. Modal analyses for five of the hybridized intrusive samples are presented in Table 8.

Hybridized rhyolite (Tr_{hy}) -- A small, narrow, discontinuous rhyolitic dike crops out near the eastern boundary of the claim block (Pl. 1), in the central portion of the study area. It intrudes both the early quartz latites and andesites of the Conejos Formation. The dike is not particularly resistant to weathering and exposures are small and discontinous.

In hand specimen, the hybridized dike is light brown to purple, similar to the color of the early quartz latite porphyry, and the two rock types are often difficult to distinguish. Field identification is facilitated by the lack of flow structure commonly demonstrated by the quartz latitic rocks, and small rounded quartz phenocrysts may be recognized in the dike rocks.

Microscopically, the rhyolitic rocks exhibit porphyritic to glomeroporphyritic textures. Phenocrysts make up about 40-50 percent of the rock. Subhedral laths of andesine (An_{26-34}), up to 5 mm

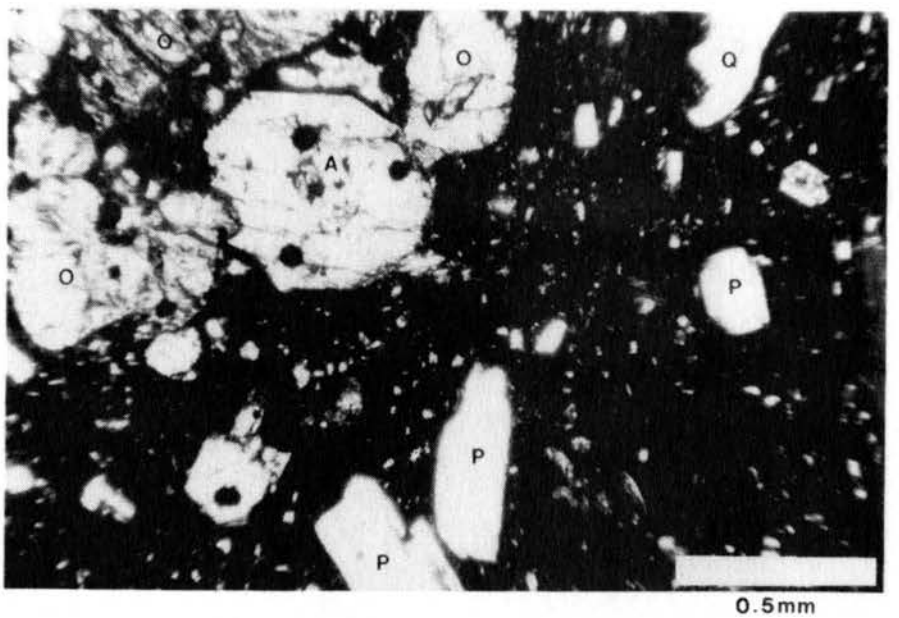

Figure 11. Photomicrograph of same sample as Figure 10 (polarized light). Phenocrysts of olivine, altered to bastite (O), augite (A), plagioclase (P), and xenocryst of quartz (Q).

Table 8. Modal analyses (volume percent) for hybridized intrusives.

	Sample				
	BS-199[1]	BS-251[1]	BS-2-26[2]	BS-2-28[2]	BS-239[2]
Groundmass	60.5	67.3	55.9	59.9	58.0
Plagioclase	24.7 An_{45}	18.6 An_{42}	26.1 An_{33}	25.9 An_{32}	29.2 An_{26-34}
Sanidine	0.9	1.7	5.2	4.9	6.5
Quartz	0.8	0.6	0.6	1.2	0.6
Tridymite	--	--	6.1	3.8	--
Biotite	1.4	1.1	1.7	2.4	2.8
Hornblende	0.4	0.3	--	--	--
Augite	5.3	4.1	--	--	--
Hypershene	1.6	1.2	--	--	--
Bastite	1.1	1.0	--	--	--
Magnetite	2.9	4.1	4.5	1.9	3.0
Calcite	tr	tr	--	--	--
Apatite	tr	tr	tr	tr	tr
Rutile	--	--	tr	tr	tr
Zircon	--	--	tr	tr	tr

[1] Tb_{hy} [2] Tr_{hy}

in their greatest dimension, comprise 25-30 percent of the rock. They are normally zoned and are often partly resorbed. Rounded grains of sanidine make up 5-6.5 percent of the rock. They are usually less than 1.5 mm in their greatest dimension and are commonly bordered by coronas or reactions rims (Fig. 12). Subhedral laths of reddish-brown biotite make up another 2-3 percent of the rock. They are up to 3.5 mm in length and have been replaced by magnetite along crystal borders and along cleavage traces. Magnetite makes up 2-4 percent of the rock, occurring as equant, discrete grains and as a replacement product. Highly embayed, rounded quartz xenocrysts comprise up to one percent of the rock. The dominant form of SiO_2, however, is as fine-grained irregular quartz grains in the felsophyric groundmass and as tridymite lining irregular shaped cavities. Accessory minerals include apatite, zircon, and rutile. Modal analyses for three of these samples are presented in Table 8.

Flow-banded rhyolite (Trfp) -- Two narrow rhyolitic dikes crop out in the southeastern and eastern portions of the study area (Pl. 1). They occur along a northeast-trending lineament, which although obscure in the field, is readily identified on high altitude aerial photographs. They intrude andesitic and rhyodacitic flows belonging to the early intermediate assemblage. No other cross-cutting relationships were observed. According to Lipman et al. (1970), their petrologic nature of 74-75 percent SiO_2, and abundant

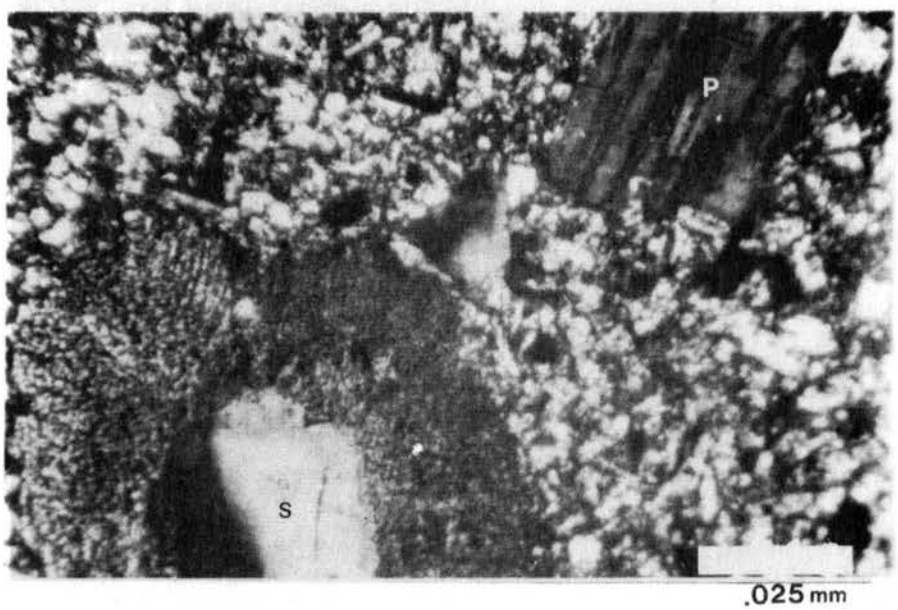

Figure 12. Photomicrograph of hybridized rhyolite (Tr_{hy}) polarized light. Phenocrysts of plagioclase (P) and sanidine (S). Note the large reaction corona surrounding the sanidine grain.

phenocrysts of alkali feldspar and quartz is almost uniquely characteristic of the rhyolites of the Hinsdale Formation.

Rocks from the rhyolite dikes are vesicular, light purple to tan, and are commonly coated by black manganese oxides. They are porphyritic with phenocrysts of quartz, sanidine, plagioclase, and biotite. Exposures commonly show good flow banding, with the prismatic phenocrysts and drawn-out vesicles indicating the direction of flow.

Microscopically, the rhyolitic rocks are porphyritic with a microcrystalline groundmass. The phenocrysts make up about 5-10 percent of the rock and include small, rounded and embayed quartz grains; subparallel, dark-brown biotite needles; subhedral, commonly Carlsbad-twinned sanidine; subhedral, sodic oligoclase (An_{14}); and magnetite grains largely altered to hematite.

JASPEROID BRECCIAS

According to Lovering (1972), jasperoid is a rock composed dominantly of quartz that has formed largely by epigenetic replacement. Jasperoids are most common in limestone and dolomite. They do, however, also occur in shale, mudstone, metamorphic rocks, and extrusive igneous rocks. Jasperoid bodies tend to be localized along faults and fracture zones, and they are often genetically and spatially related to siliceous igneous intrusives.

The Tracy Canyon area is characterized topographically by three prominent and several smaller subsidiary jasperoid plugs

(Fig. 13 and Pl. 1). The host rocks for the epigenetic replacement solutions were dominantly quartz latite breccias. The volcanic breccias were probably formed by the sudden venting of volatiles along localized zones of weakness or low pressure, such as faults and fractures. Channelways created by these structural zones provided avenues for the subsequent hydrothermal solutions. An alternative hypothesis is that the breccias represent a sheet-like mass, possibly orginating from a detachment fault. However, the apparent structural control indicated by the altered rocks, and the pipe-like nature of the jasperoid breccias are difficult to explain utilizing this argument. The primary source of silica in the jasperoid bodies cannot be conclusively established. In addition to the silica derived from the epigenetic silica-rich solutions, the silica released by the reactions between the hypogene solutions and the silicate wall-rock minerals may have also been an important source.

Although porphyritic volcanic textures in many of the jasperoids have been preserved, the volcanic breccias, for the most part, have been entirely replaced by SiO_2. Table 9 compares the composition of 10 representative jasperoid samples (from Lovering, 1972) to the composition of Tracy Canyon jasperoids.

There is no obvious siliceous igneous intrusive genetically and spatially related to the jasperoids in the study area. The altered rocks in the study area are, however, crudely distributed about the

Figure 13. View of pipe-like jasperoid body in the fog.

Table 9. The observed range and average concentrations, in percent, of the 8 commonly reported oxides for 10 representative jasperoid samples (Lovering, 1972), compared to jasperoids from the Tracy Canyon area.

	10 representative jasperoid samples (Lovering, 1972)		Tracy Canyon jasperoid samples	
	Range	Average	Range	Average
SiO_2	80.0 - 97.0	92.8	75.0 - 98.0	91.6
TiO_2	0.0 - 0.8	0.2	0.2 - 1.7	1.0
Al_2O_3	0.3 - 4.0	1.4	0.5 - 13.2	4.2
FeO	0.2 - 7.0	0.4	0.3 - 5.1	1.6
MgO	0.0 - 1.0	0.4	0.0 - 0.5	0.1
CaO	0.0 - 1.0	0.2	0.1 - 2.8	0.4
Na_2O	0.0 - 0.3	0.1	0.1 - 2.0	0.4
K_2O	0.1 - 1.0	0.3	0.1 - 3.6	0.9

granodiorite stock and the jasperoid bodies may be genetically related to this intrusive. The absence of an igneous intrusive genetically and spatially related to the jasperoids could also imply the existence of a deep-seated siliceous intrusive.

The jasperoid outcrops in the Tracy Canyon area vary widely in physical appearance. The unoxidized varieties generally range from white through various shades of gray to dark brown. Oxidized outcrops commonly exhibit various shades of yellow, orange, pink, and red. In addition, the jasperoid bodies commonly exhibit iron and manganese oxides as surface stains and fracture coatings. Individual jasperoid bodies range in size from pods less than one meter in diameter to masses 150 meters in their greatest dimension. Texturally, the jasperoid rocks range from dense and relatively homogenous to cavernous and highly brecciated. The vugs in the cavernous jasperoids lack any preferred orientation and may be lined with crystals of quartz and calcite, and sometimes specular hematite or pyrite. Fragments in the jasperoid breccias are angular and range in size from several centimeters to less than one millimeter in their greatest dimension (Fig. 14).

Microscopically, the jasperoids exhibit a very fine-grained xenomorphic granular to "jigsaw-puzzle"[1] texture (Fig. 15). Quartz is the major constituent and occurs as highly irregular, tightly interlocking grains less than 1 mm in their greatest dimension. In the

[1] As defined by Lovering (1972).

Figure 14. Outcrop of jasperoid breccia showing variation of size and angular nature of breccia fragments.

Figure 15. Photomicrograph of a jasperoid breccia sample exhibiting an xenomorphic granular to "jigsaw-puzzle" texture.

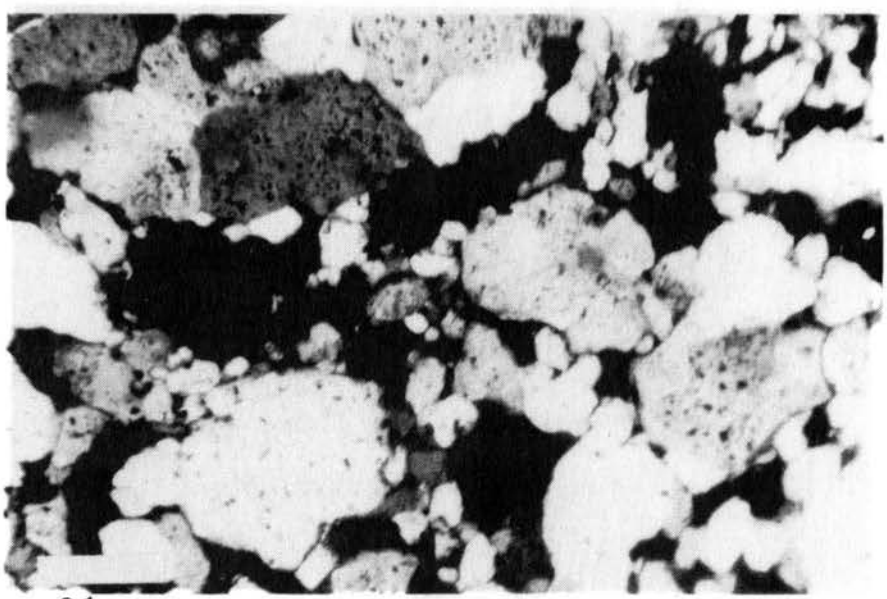
0.1 mm

oxidized jasperoids, bright orange crystalline goethite occurs as irregular masses associated with amorphous dark brown limonite. The iron oxides occur with quartz in late stage veinlets and also along fractures and breccia fragment boundaries. Minor amounts of pyrite are visible in many of the unoxidized jasperoid breccias. Accessory minerals include allophane, alunite, and zircon. Allophane is a common but minor constituent of the jasperoids and occurs as tiny inclusions embedded in the quartz grains. The zircon occurs as small rounded detrital grains, remnants of the volcanic host.

Molybdenite was not identified, in any of the jasperoid samples or polished sections. Several of the jasperoids, however, contain anomalous molybdenum values up to 100 ppm. Values of this magnitude in the unoxidized samples probably indicate the presence of molybdenite.

STRUCTURE

GENERAL STATEMENT

Geologic sections across the area is shown in Plate 2. The major structural features of the Tracy Canyon area are: (1) relatively flat lying to gently dipping flows and flow breccias; (2) small horst and graben structures in the central portion of the study area; (3) short, vertical or steeply dipping branch faults and a northwest-trending strike-slip fault; and (4) a major structural lineament, expressed in the study area by flow-banded rhyolite dikes.

VOLCANICS DIPPING GENTLY TO THE NORTHEAST

Flows in the study area are relatively flat lying with gentle dips ranging between 10 and 20 degrees, most often to the northeast. Around the upthrown fault block in the central part of the area, however, the rocks dip, sometimes more steeply, to the northwest. According to Lipman et al. (1970), as the episode of violent ash-flow eruptions came to a close, the eastern San Juan Mountains, in response to the development of the Rio Grande Rift, were faulted, broadly warped, and tilted to the east. The preponderance of eastward-dipping rocks in the study area is, most likely, an expression of this event.

SMALL HORST AND GRABEN STRUCTURES

North- and southwest-trending faults in the central part of the study area bound small horst and graben structures. They have lengths of up to two kilometers and vary in width from about 60 meters to over 600 meters. In most instances, neither the ages of faults nor the amount of vertical displacement along them can be determined. However, vertical displacements on the northwest-trending faults bordering the downthrown basaltic andesite-capped block (Pl. 1) and the approximate ages of these faults can be estimated. The composition and stratigraphic position of the basaltic andesites in the central and western portions of the thesis area suggest they are equivalent to the Hinsdale Formation of Larsen and Cross (1956). If this is the case, the northwest-trending faults must be Miocene or younger in age. The position of the unfaulted basaltic andesites to the west implies a vertical displacement along the faults of approximately 200 meters (Pl. 2).

These faults were probably activated (or reactivated) in the late Tertiary in response to regional eastward tilting of the terrain and regional crustal extension associated with development of the Rio Grande Rift.

FAULTS

Faults in the study area tend to be expressed as valleys and topographic breaks. As a result, they are commonly covered by talus

and alluvium and are often difficult to detect. Undoubtedly, some less obvious faults were not identified.

The general style of faulting and its relation to hydrothermal alteration is shown in Figs. 18-22. The faults in the study area tend to be short (less than three kilometers long) and have straight or gently curved traces. Angular breaks and branch faults are common. Vertical, or steeply-dipping normal faults commonly bound or are otherwise associated with small horsts and graben. A northwest-trending strike-slip fault offsets Conejos Formation andesites and quartz latites in the northeastern portion of the study area, with a relative displacement of approximately 300 meters (Pl. 1). The localization of Conejos Formation equivalent intrusives along recognized faults which offset Hinsdale Formation volcanics, and the apparent displacement of hydrothermally altered rocks suggest histories of recurrent movement. Most likely, these faults were initiated with the episode of middle and late Oligocene volcanism, and reactivated in the late Cenozoic as a response to regional crustal extension.

STRUCTURAL LINEAMENT

Flow-banded rhyolitic dikes within the study area are the expression of a northeast-trending lineament that intersects the Beidell volcanic center (Crystal Hill mining district), 13 kilometers to the southwest, and the Klondike mining district, 16 kilometers to the

northeast. The petrologic nature of the rhyolitic dike rocks (high SiO_2 content, abundant phenocrysts of alkali feldspar and quartz with fewer of plagioclase) is almost uniquely characteristic of the rhyolites of the Hinsdale Formation (Lipman et al., 1970). Displacement along this structural feature is undetermined, but it is, undoubtedly, an expression of an extensional feature activated (or reactivated) during the development of the Rio Grande Rift.

HYDROTHERMAL ALTERATION AND MINERALIZATION

GENERAL STATEMENT

Hydrothermal alteration extends over an area of approximately 13 square kilometers, centered about an area of vertical or high-angle normal faults and small horst and graben structures, in the central part of the study area. Three alteration zones have been recognized (Pl. 1): (1) a high-silica alteration zone, composed primarily of jasperoid rocks in the central zones of breccia pipes; (2) argillized breccias and volcanics (advanced argillic zone, as defined by Hemley and Jones, 1964) that irregularly envelope the high-silica rocks; and (3) non-brecciated, silicified quartz latites. Within the study area, all lavas of the early intermediate assemblage and their hypabyssal equivalents show some degree of hydrothermal alteration. The early quartz latites, however, are most severely affected.

In the field, the advanced argillic and high-silica alteration zones were distinguished somewhat arbitrarily by the ease with which altered rocks could be scratched by a knife blade. The boundary between the two alteration zones is gradational. Highly-silicified rocks often contain abundant kaolinite, and rocks of the advanced argillic zone may contain large quantities of hydrothermal quartz.

HIGH-SILICA ALTERATION ZONE

The high-silica zone is comprised principally of jasperoid breccias. Some highly-silicified rocks containing moderate amounts of kaolinitic clays have been included in this alteration zone. Quartz is the dominant alteration product, and kaolinite is common in subordinant amounts. Outcrops are often coated by red and orange iron oxides, black manganese oxides, and occasional iridescent oxide stains. The high-silica rocks are resistant to erosion and protrude as chimney- or pipe-like structures above the unaltered and brecciated volcanics (Fig. 13). Chemically, these rocks reflect extensive leaching of base cations--aluminum, magnesium, calcium, sodium, and potassium--and introduction of silica. In the unoxidized high-silica breccias, small veinlets and scattered disseminations of pyrite are common, and minor amounts of molybdenite are also present.

ADVANCED ARGILLIC ALTERATION ZONE

The advanced argillic alteration zone consists of altered breccias and volcanics. Contacts with the silicified breccias and the unaltered and relatively unfractured country rocks tend to be gradational. In hand specimen, the rocks are grayish-white to yellow. Kaolinite is the dominant alteration product. Quartz is common in subordinant amounts, occurring as irregular veinlets and as cryptocrystalline silica both in the breccia fragments and in the groundmass. Montmorillonite, sericite, jarosite, alunite, and leucoxene are sparse

constituents of the advanced argillic assemblage. Rocks of the advanced argillic alteration zone are less resistant to weathering and commonly form the slopes surrounding pipe-like jasperoid breccias. Argillized rocks also occur as irregular pods and lenses, commonly associated with faults and fractures. The major chemical changes involved in argillization of rocks are leaching of magnesium, calcium, and sodium, and introduction of silica. Aluminum and potassium remain relatively unchanged. Pyrite occurs in veinlets with hydrothermal quartz and as scattered disseminations. Molybdenite, although not recognized, probably occurs in small amounts, as indicated by Mo contents of up to 200 ppm.

SILICIFIED QUARTZ LATITES

Non-brecciated, silicified quartz latites define a third alteration zone. These rocks are confined predominantly to a small knob in the north-central part of the study area, and to an apparent early quartz latite vent area in the northeastern corner of the study area (Pl. 1). Hand specimens generally appear fresh, and biotite and plagioclase phenocrysts are unaltered. Microscopic inspection, however, reveals small veinlets of quartz and a mottled, slightly argillized looking groundmass. Contacts with the advanced argillic breccias and volcanics, and with the unaltered early quartz latites, tend to be gradational. Chemically, the rocks reflect introduction of SiO_2 and a slight leaching of CaO. The average SiO_2 content of the

unaltered quartz latites is approximately 68 percent, whereas the silicified quartz latites average about 73 percent SiO_2. The invading silicic solutions may have partially decomposed plagioclase feldspars in the cryptocrystalline groundmass, and in so doing, liberated CaO. No sulfide minerals have been identified in any silicified quartz latite sample.

THE HYDROTHERMAL ALTERATION PROCESS

Hydrothermal alteration has been interpreted to have resulted from hydrogen ion metasomatism as described by Hemley and Jones (1964). Fig. 16 depicts hypothetical diffusion gradients and alteration zones for hydrolytic-type alteration of silicate rocks. The pattern of alteration is one of decreasing hydrogen ion activity away from the center of the major fluid conduit. Development of the sericite-quartz zone is characterized by extensive leaching of magnesium, calcium, sodium, potassium, and aluminum and introduction of an equivalent amount of ionized hydrogen. The argillic zone reflects removal of calcium, sodium, and magnesium and introduction of hydrogen. Aluminum and potassium (not shown on the diagram) remain relatively constant.

According to Hemley and Jones (1964), a dominant alteration process in the argillic zone is the hydrolytic decomposition of andesine to kaolinite.

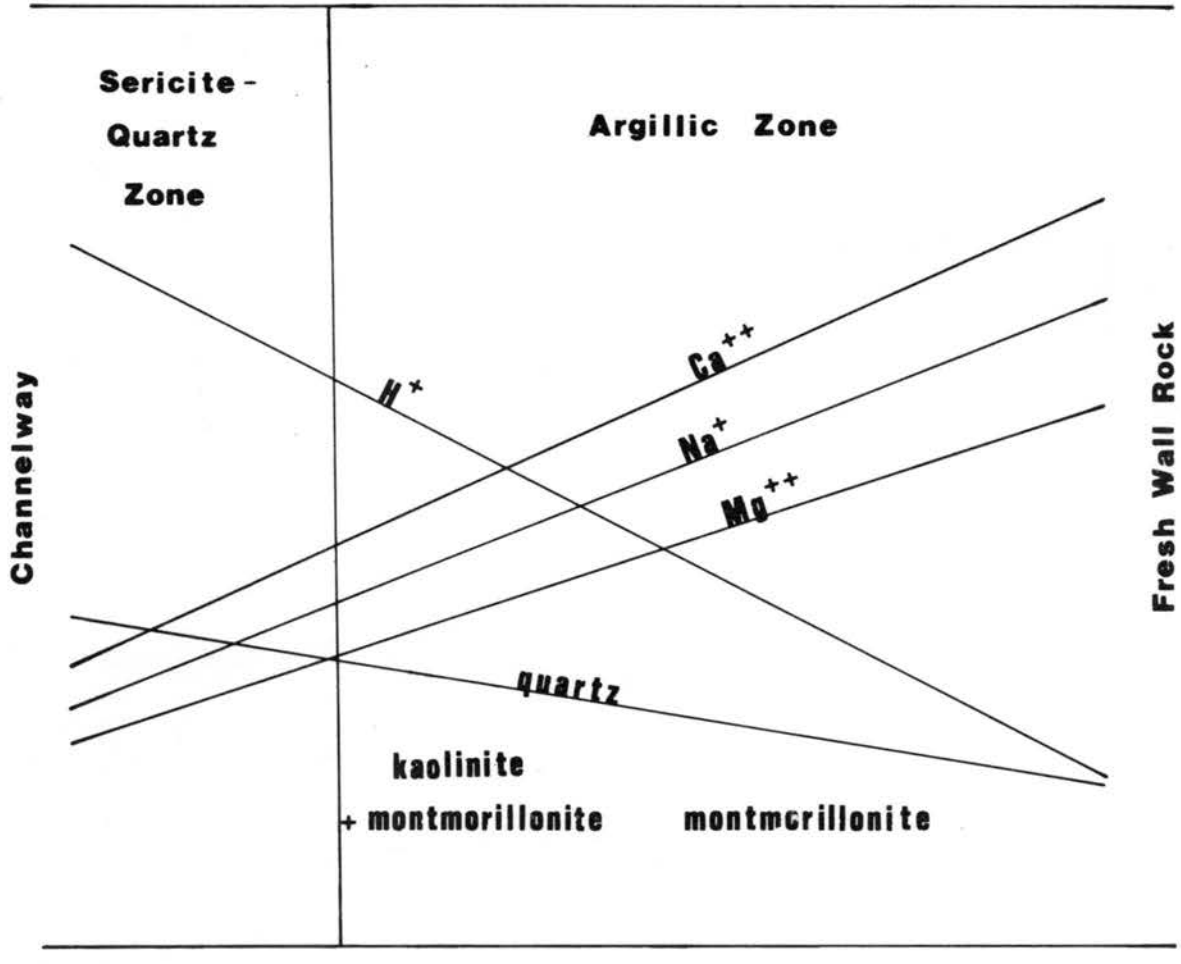

Figure 16. Hypothetical diffusion gradients and alteration zones for hydrolytic-type alteration of silicate rocks. Modified from Hemley and Jones (1964).

$$\underset{\text{andesine}}{Na_2CaAl_4Si_8O_{24}} + 4H^+ + 2H_2O \rightleftharpoons \underset{\text{kaolinite}}{2Al_2Si_2O_5(OH)_4} + 4SiO_2 + 2Na^+ + Ca^{+2}$$

In the sericite-quartz alteration zone, hydrogen ions are consumed in leaching Al^{+3} and the ultimate product may be nothing more than a porous mass of quartz.

$$\underset{\text{kaolinite}}{Al_2Si_2O_5(OH)_4} + 6H^+ + 3.5H_2O \rightleftharpoons \underset{\text{quartz}}{2SiO_2} + 5H_2O + 2Al^{+3}$$

The chemical changes for progressively altered quartz latites from Tracy Canyon are depicted in Fig. 17. Other than the fact that sericite is not an important phase in the alteration assemblage, the salient features of Hemley and Jones' (1964) hypothetical model are well displayed, and the previously established chemical reactions are probably applicable.

Many of the jasperoid breccias occur along faults recognized in the field and the occurrence of others is undoubtedly controlled by similar, less obvious structures that have acted as channelways for the altering hydrothermal solutions. Core taken from shallow drill holes in the jasperoid pipes indicates that the highly-silicified rocks and breccias are prevalent only at shallow depths. With increasing depth, these give way to an advanced argillic assemblage characterized by less intense base cation leaching and hydrogen ion metasomatism. The general pattern of hydrothermal alteration is, therefore,

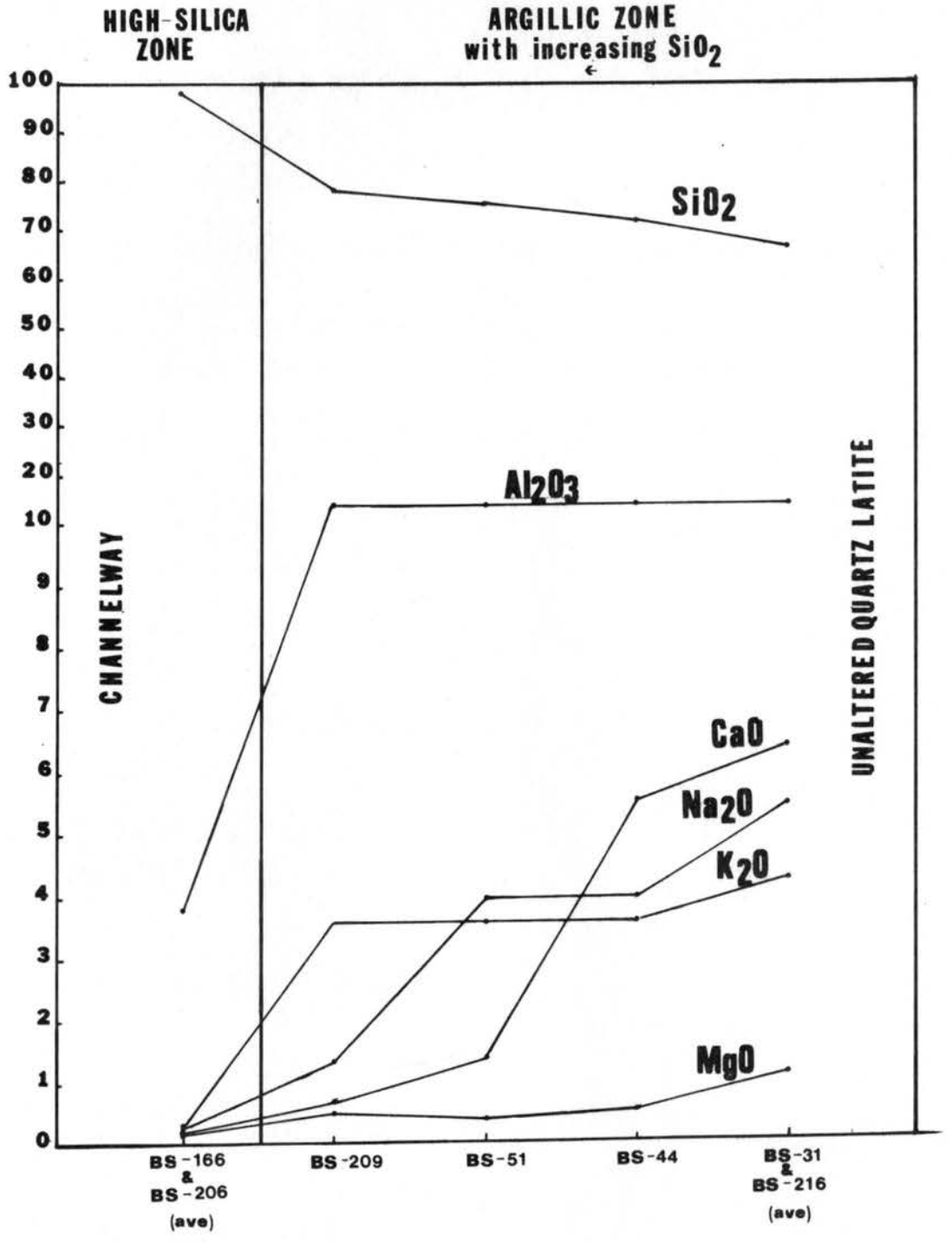

Figure 17. Chemical changes for progressively altered quartz latites in the Tracy Canyon area. BS-166 and BS-206, jasperoid breccia samples; BS-209, advanced argillic breccia sample; BS-51 and BS-44, argillized quartz latite samples; and BS-31 and BS-216, unaltered quartz latites. The Al_2O_3 curve may, in part, reflect a poor analytical sensitivity for Al.

one of decreasing hydrogen ion metasomatism away from the jasperoid breccias, the major sources of fluid emanations.

TRACE METAL DISTRIBUTION

GENERAL STATEMENT

Two hundred-eighty rock chip samples were collected in the field. Emission spectrographic analyses of 35 elements for each of the rock chip samples were provided by W. A. Bowes and Associates. Maps showing the distribution of anomalous concentrations of Cu, Pb, Zn, Mo, and As are presented in Figs. 18-22. Sample locations are shown on Pl. 3, and the values for Cu, Pb, Zn, Mo, and As are listed in the Appendix, Table A-1. Histograms showing concentrations of Cu, Pb, Zn, and Mo in rocks from the Tracy Canyon area are included in Fig. 23. Mean concentrations of Cu, Pb, Zn, and Mo in different rock and alteration types are indicated by the histograms in Fig. 24.

THE DISTRIBUTION OF COPPER

Rocks collected from the study area range in Cu content from 10-200 ppm (Fig. 23). The highest Cu value, 200 ppm, is for an advanced argillic breccia sample (Fig. 18 and Table A-1). The next highest values, 70-100 ppm, are most common in the andesitic flow and dike rocks. Hawkes and Webb (1962) give the average copper content of igneous rocks as 70 ppm. The average Cu concentration of the andesitic rocks in the study area (40 ppm) is identical to the

Figure 18. Cu anomaly distribution map. High-silica rocks indicated by solid lines. Dashed lines indicate rocks of advanced argillic zone and shaded pattern indicates silicified quartz latites. Triangles denote breccias.

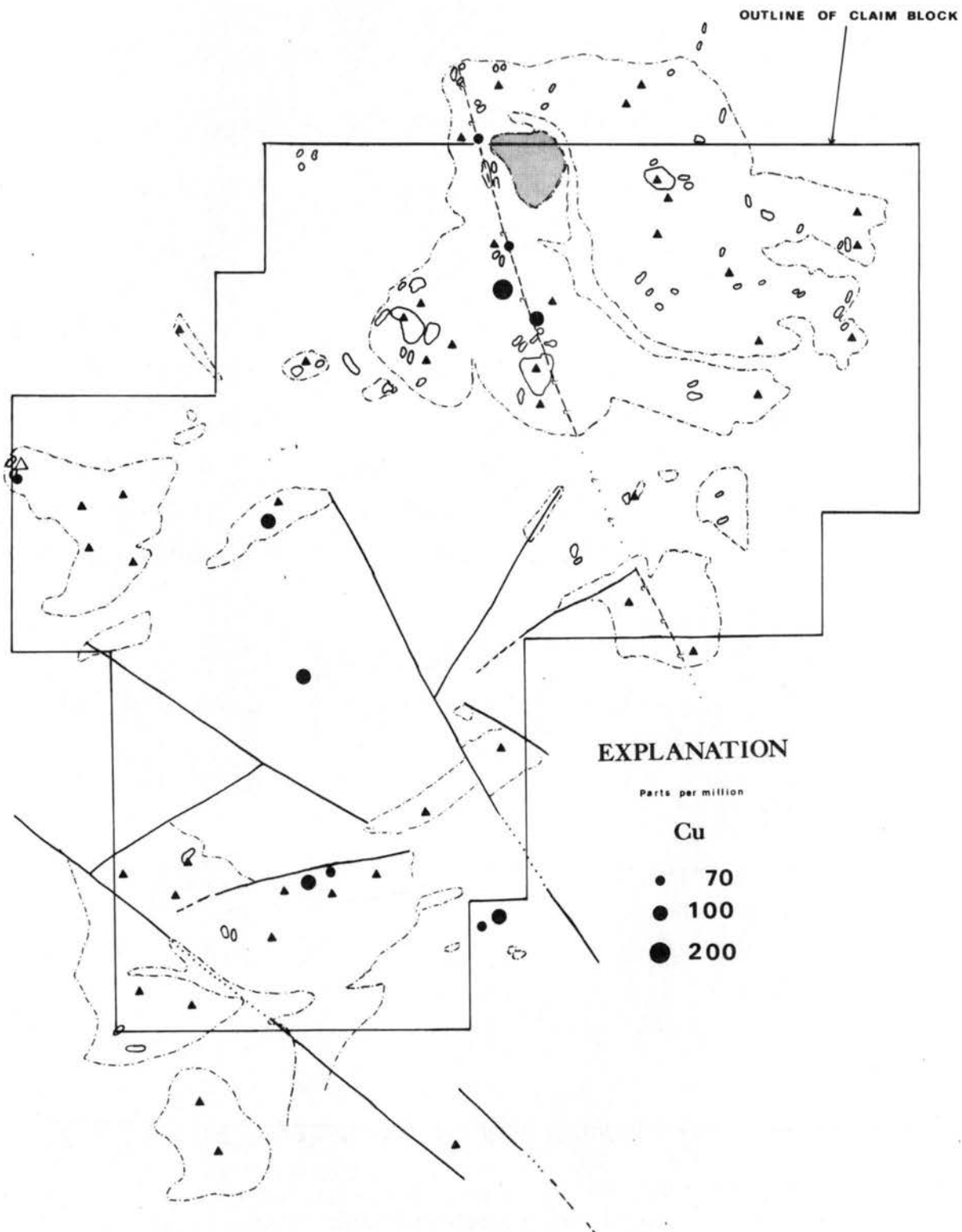
OUTLINE OF CLAIM BLOCK
EXPLANATION
Parts per million
Cu
70
100
200

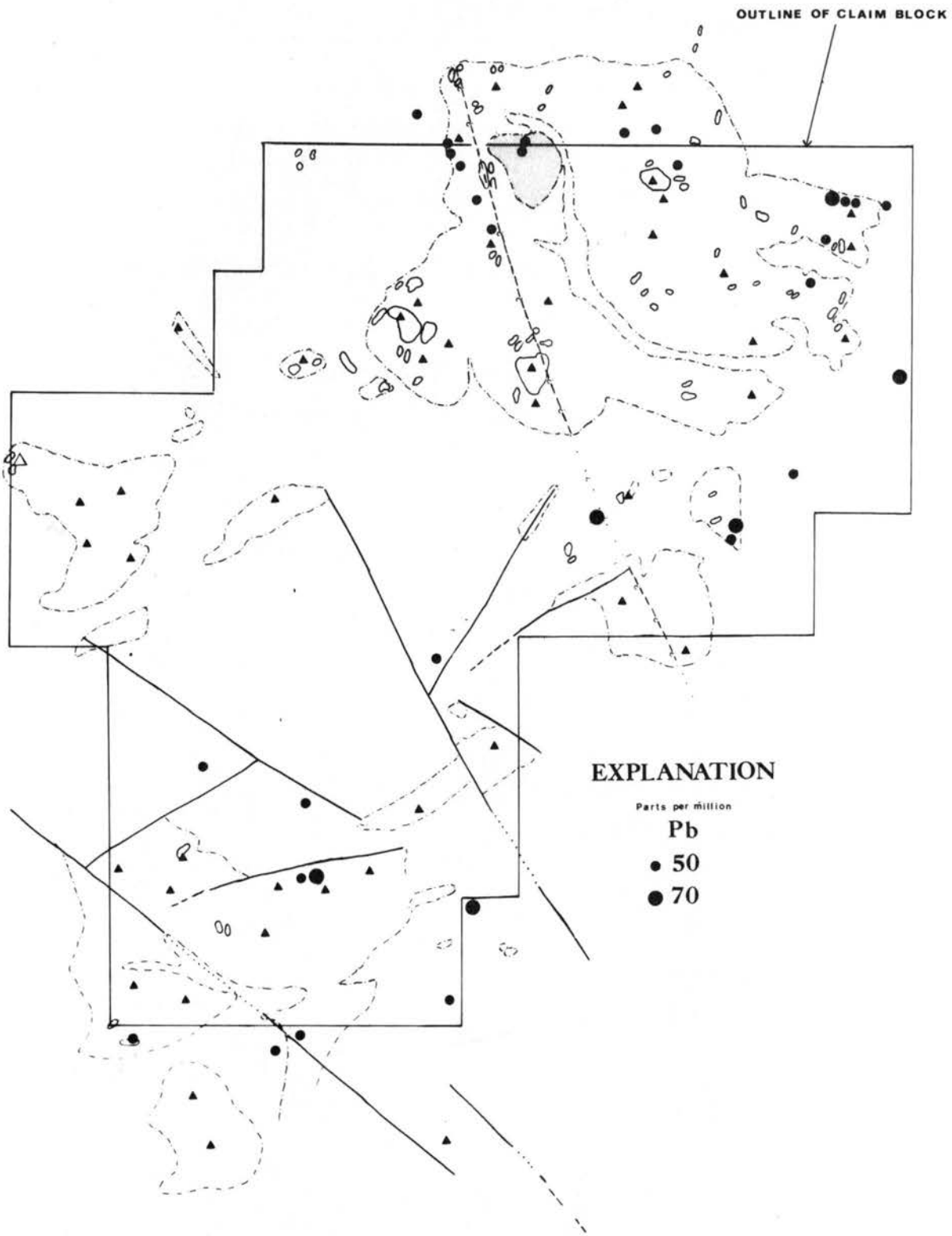

Figure 19. Pb anomaly distribution map. High-silica rocks indicated by solid lines. Dashed lines indicate rocks of advanced argillic zone and shaded pattern indicates silicified quartz latites. Triangles denote breccias.

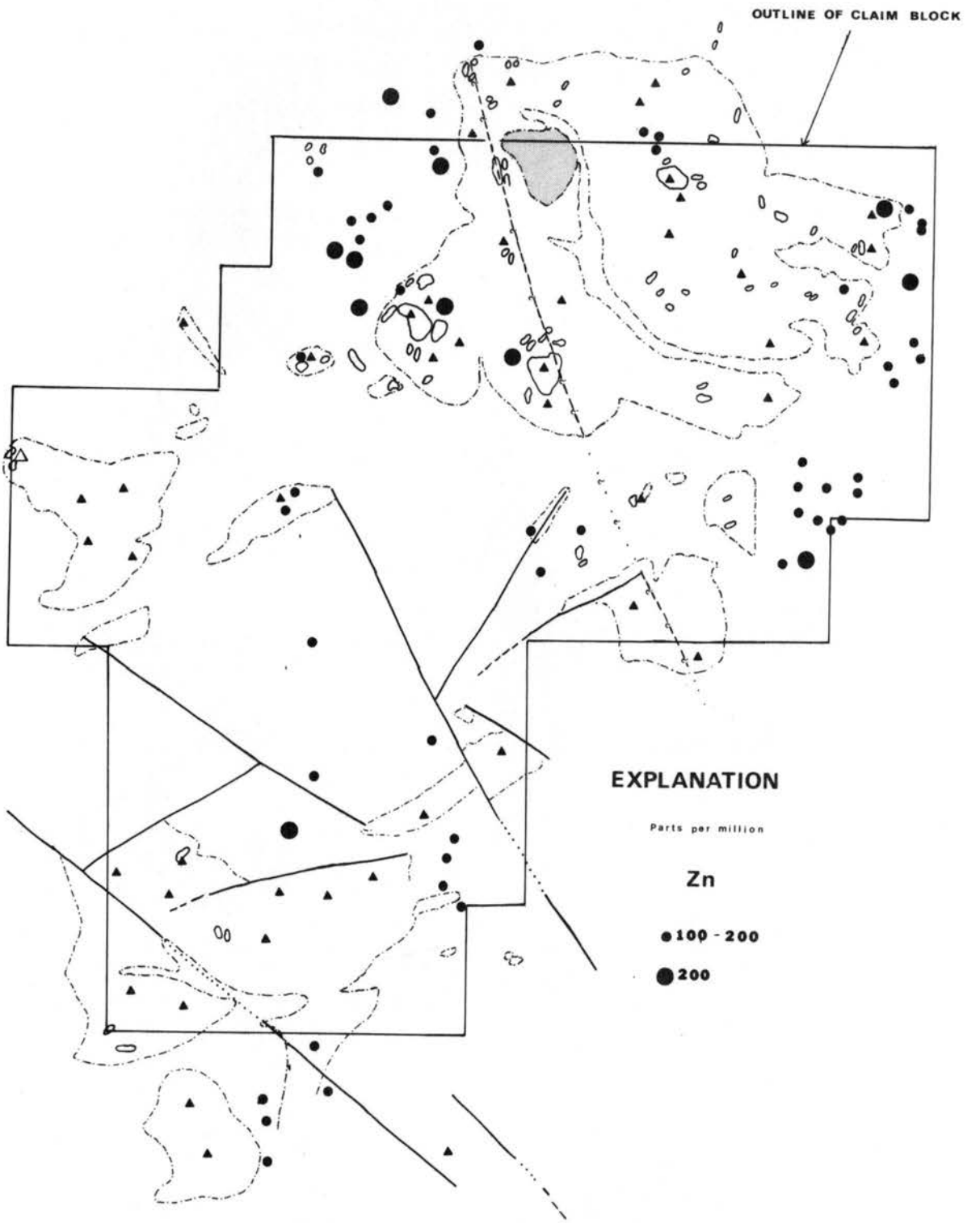

Figure 20. Zn anomaly distribution map. High-silica rocks indicated by solid lines. Dashed lines indicate rocks of advanced argillic zone and shaded pattern indicates silicified quartz latites. Triangles denote breccias.

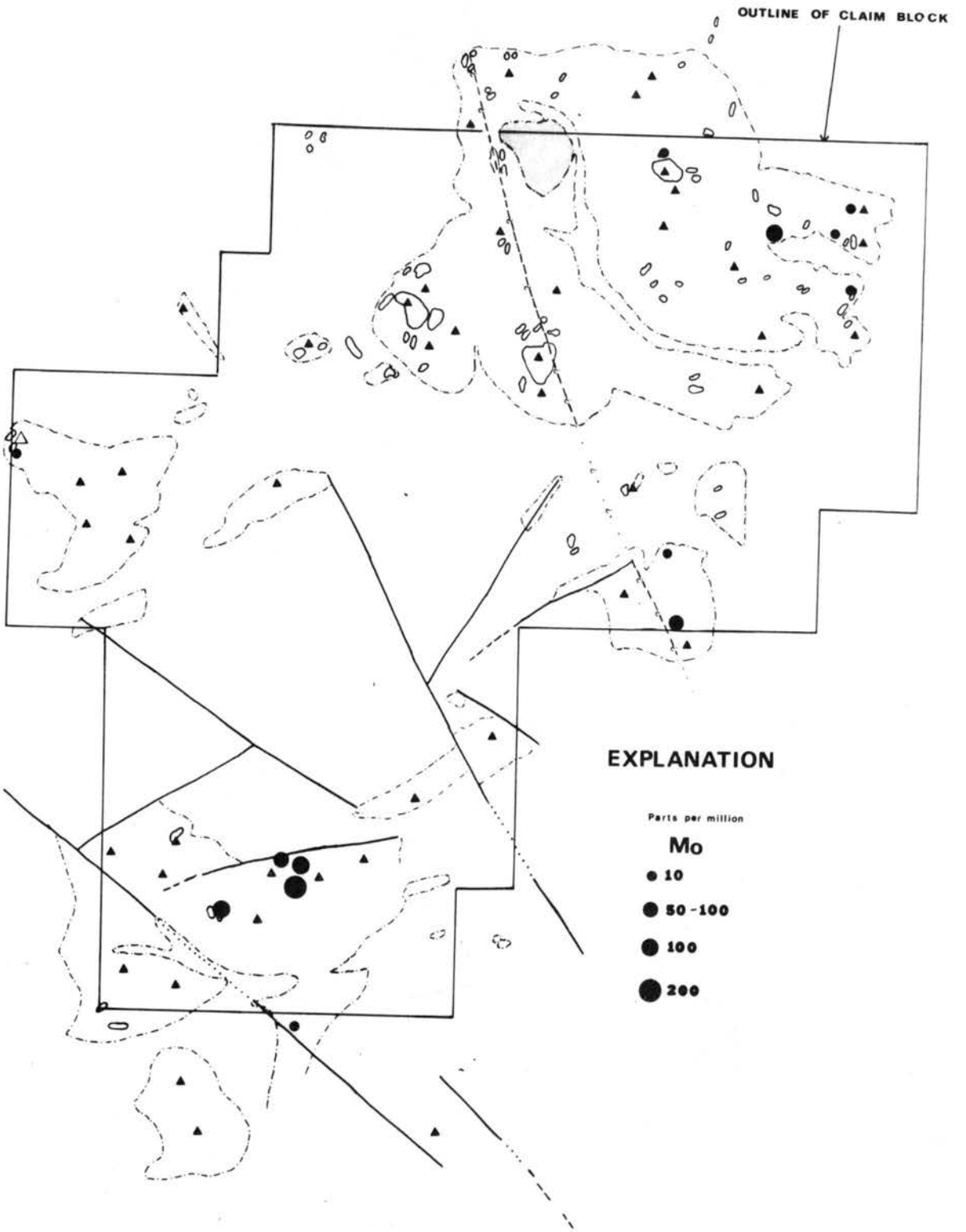

Figure 21. Mo anomaly distribution map. High-silica rocks indicated by solid lines. Dashed lines indicate rocks of advanced argillic zone and shaded pattern indicates silicified quartz latites. Triangles denote breccias.

Figure 22. As anomaly distribution map. High-silica rocks indicated by solid lines. Dashed lines indicate rocks of advanced argillic zone and shaded pattern indicates silicified quartz latites. Triangles denote breccias.

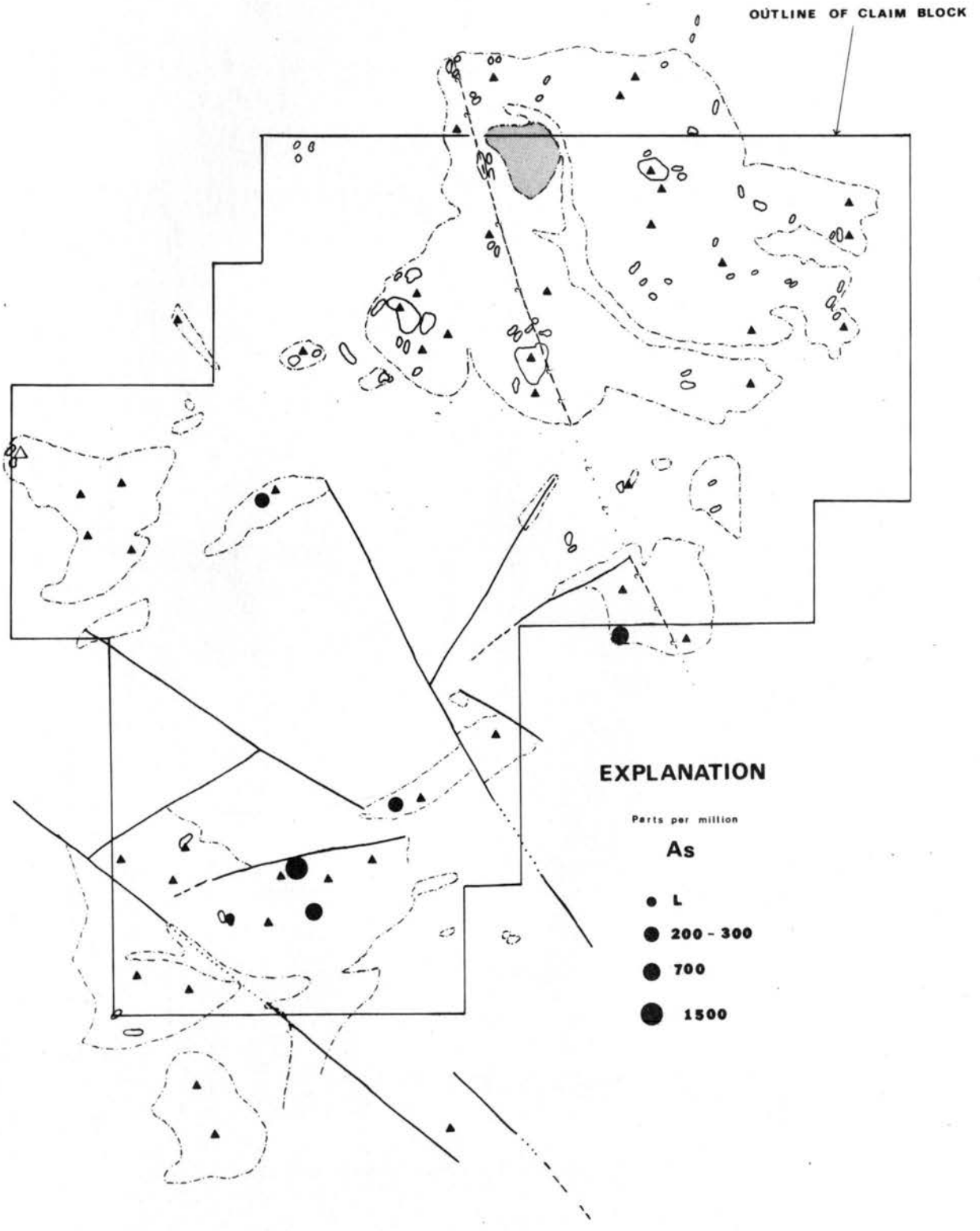
OUTLINE OF CLAIM BLOCK
EXPLANATION
Parts per million
As
L
200 - 300
700
1500

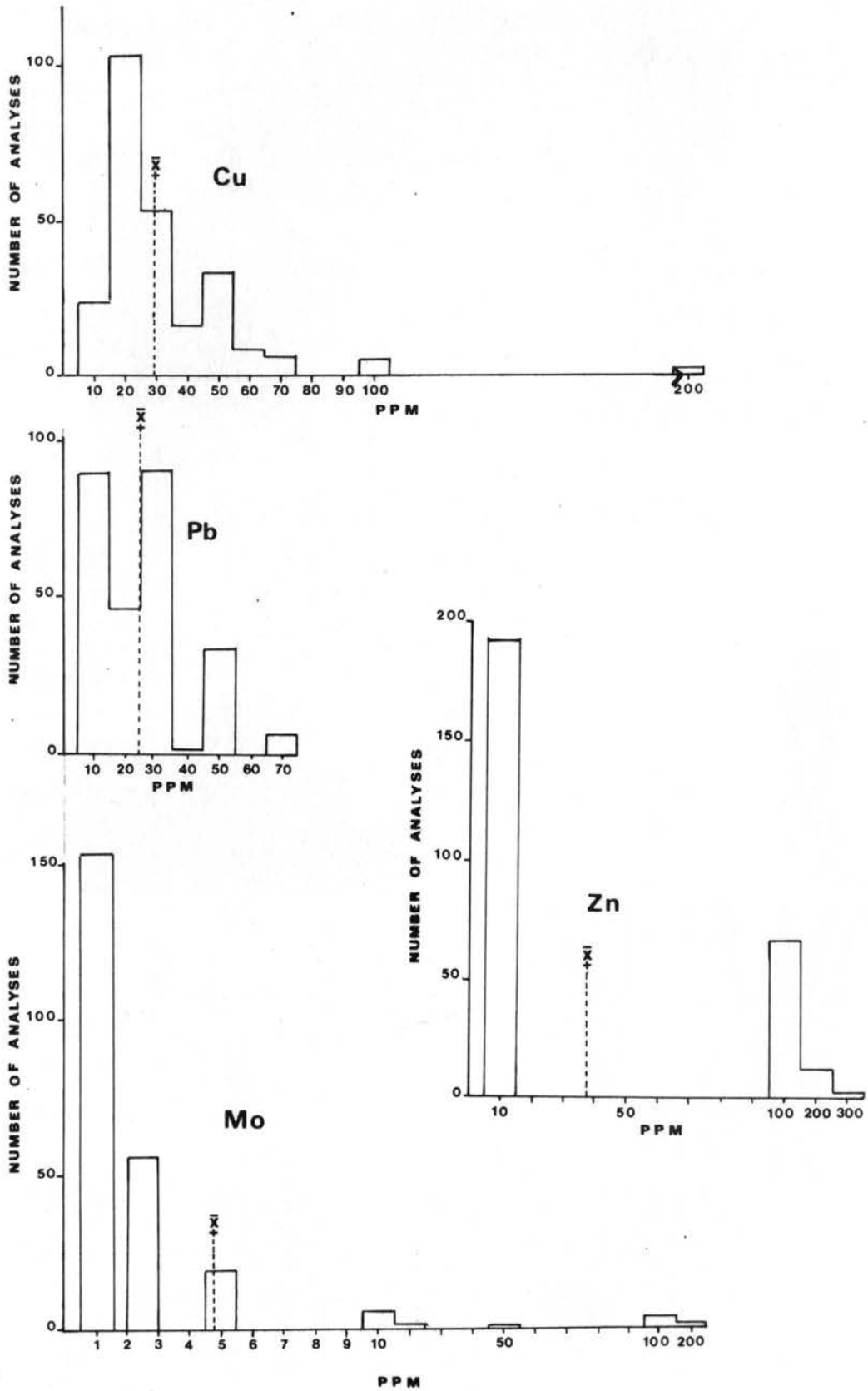

Figure 23. Histograms showing frequency distributions for analyses of Cu, Pb, Zn, and Mo. $\bar{X}$ indicates arithmetic mean.

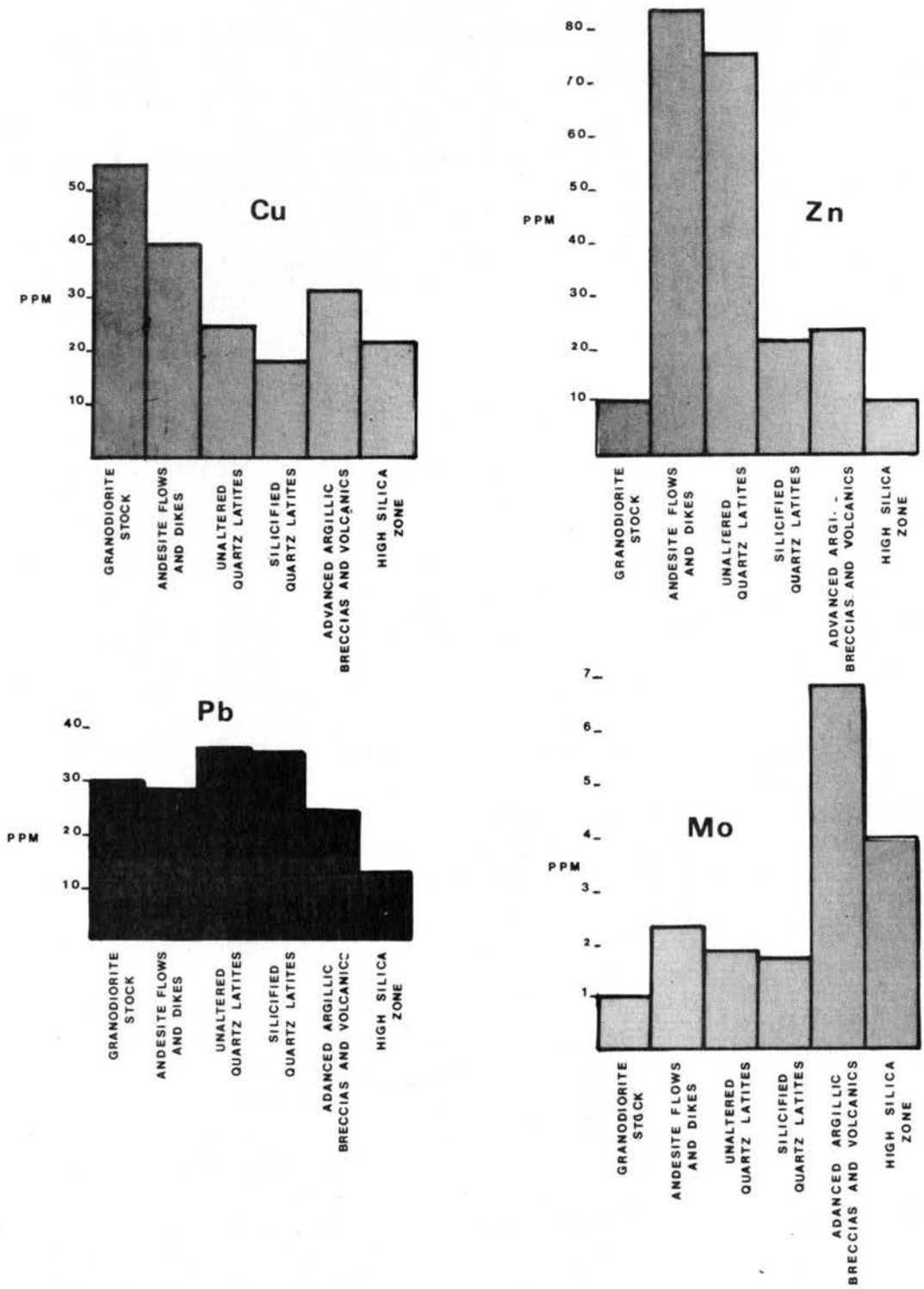

Figure 24. Histograms showing mean concentrations of Cu, Pb, Zn, and Mo in different rock and alteration types.

value given by Ahrens (1968) for average andesite. Copper contents of the order of 200 ppm, in the advanced argillic rocks, probably indicates the presence of chalcopyrite. The source of the anomalous Cu could have been either Cu leached from the country rocks, or the Cu might have been a component of the "original" hydrothermal solutions.

THE DISTRIBUTION OF LEAD

Pb values range from below the detection limit (10 ppm) to 70 ppm. Values of 30 ppm or less prevail (Fig. 23). The highest Pb concentrations occur in unaltered and silicified quartz latites and in rocks from the advanced argillic alteration zone (Fig. 19 and Table A-1). Hawkes and Webb (1962) give the average Pb content of igneous rocks as 16 ppm. The distribution of Pb apparently reflects slight leaching in the advanced argillic alteration zone and intense leaching in the high-silica zone.

THE DISTRIBUTION OF ZINC

Zn values range from below the detection limit (10 ppm) to 300 ppm (Fig. 23). The distribution of Zn in Fig. 23 is somewhat misleading because the value 100 ppm was arbitrarily assigned to those samples in which Zn was detected but was below the lower limit of determination, and 10 ppm was assigned to samples in which Zn was not detected. In the majority of the analyses, Zn was either not

detected or was below the lower limit of determination (Table A-1). The highest Zn value (300 ppm) belongs to an advanced argillic breccia sample (Fig. 20 and Table A-1). Zn values of 200 ppm are found both in advanced argillic zone rocks and in unaltered volcanics. According to Hawkes and Webb (1962), the average Zn content in igneous rocks is 80 ppm. The behavior of Zn is best illustrated in Fig. 24, which shows that Zn is strongly depleted in the altered rocks relative to the unaltered volcanics, and high-silica rocks contain much less Zn than do advanced argillic rocks. Anomalous concentrations of Zn in the advanced argillic zone probably represent accumulations derived by earlier strong leaching of rocks in the high-silica alteration zone.

THE DISTRIBUTION OF MOLYBDENUM

Mo values range from below the lower limit of determination (5 ppm) to 200 ppm (Fig. 23). In most analyses, Mo was either not detected or was below the limit of determination. Hawkes and Webb (1962) give the average Mo content of igneous rocks as about 1.7 ppm. The highest value, 200 ppm, comes from a single advanced argillic breccia sample (Fig. 21 and Table A-1). Mo values of 100 ppm are found in rocks from both the high-silica and advanced argillic zones, and anomalous Mo concentrations of 10 ppm or greater are restricted to high-silica and advanced argillic rocks. Most likely, the Mo was introduced by the invading hydrothermal solutions, and it is unlikely

that anomalous concentrations of Mo resulted from leaching of the wallrocks.

THE DISTRIBUTION OF ARSENIC

As values range from below the detection limit (200 ppm) to 1500 ppm (Fig. 23). In most of the samples from the study area As was not detected. According to Hawkes and Webb (1962), the average As content of igneous rocks is about 2 ppm. Samples in which As was detected are restricted to rocks of the high-silica and advanced argillic alteration zones (Fig. 23 and Table A-1). Most likely, the As, like the Mo, was derived from the hydrothermal solutions and not from the altered volcanic wallrocks.

SUMMARY AND CONCLUSIONS

The highest Cu, Pb, and Zn values are associated with rocks of the advanced argillic alteration zone. Highest mean concentrations, however, are restricted to unaltered quartz latites and andesites. The anomalous concentrations of Pb, Zn, and probably Cu in the advanced argillic rocks were most likely introduced by mobilization of these elements from rocks in the high-silica alteration zone.

Anomalous concentrations of Mo and As are associated exclusively with the advanced argillic and high-silica alteration zones. Mo and As are chalcophile elements and, unlike Cu, Pb, and Zn, are not readily incorporated into the crystal lattices of most silicate minerals.

The anomalous Mo and As concentrations in the advanced argillic breccias and volcanics are difficult to account for by leaching of the volcanic wallrocks. More likely, these elements were introduced with the invading hydrothermal solutions.

ALTERATION GEOCHEMISTRY

CORRELATION COEFFICIENT MATRICES

The correlation coefficient is a useful tool that can be utilized in searching for geochemically meaningful relations among various elements. When large masses of geochemical data are available they can be particularly valuable for discerning pathfinder elements that can be used as guides in the search for ore deposits. Correlation coefficients can also be applied to hydrothermal alteration studies where it is important to distinguish the relative behavior between different elements.

The correlation coefficient (r) is calculated by:

$$r = \Sigma XY - \frac{(\Sigma X)\ (\Sigma Y)}{n} \Big/ \sqrt{(X-\overline{X})^2\ (Y-\overline{Y})^2}$$

It can be defined as simply the measure of the mutual relationship between two variables. The value r always lies between -1 and +1. Positive r values indicate a tendency for two variables to increase together, whereas negative r values signal inverse variation of the parameters tested. An r value of ± 1 indicates a perfect linear relation between two variables and an r value of 0 denotes no relation between two variables. For a more comprehensive discussion of the derivation and application of correlation coefficients, the reader is referred to Krumbein and Graybill (1965) or any standard statistics text.

Correlation coefficient matrices have been computed from emission spectrographic analyses of rocks from the high-silica, advanced argillic, and silicified quartz latite alteration zones, and are included in Figs. 25, 29, and 30. Coefficient values not significant at the .05 significance level have been listed as zero.

Correlation Coefficient Matrix for the High-Silica Alteration Zone

The matrix in Fig. 25 is based on 63 emission spectrographic analyses. Zn was not detected in any of the samples and is not included in the matrix. The most conspicuous linear relationships are those exhibited by Pb, Sr, and Na. The plot in Fig. 26 illustrates the linear relationship between Na and Pb. The mutual relationships demonstrated by these elements can easily be explained by evaluating their crystal chemistry and geochemical behavior. Sr and Na are lithophile elements, concentrated in the feldspars in silicate rocks; Pb is dominantly chalcophile in nature, and is concentrated in residual magmatic solutions. However, Pb also exhibits some lithophile tendencies, and because Pb and K have similar ionic radii (Pb^{+2} 1.20Å, K^{+} 1.33Å), Pb is able to substitute for K in feldspars. According to Goldschmidt (1958), Pb may substitute for K in amounts up to 100 ppm in high-temperature potash feldspars. Potassium correlation coefficients were not calculated because K content was determined for only a limited number of samples. A plot of the available K analyses,

	Cu	Pb	Mo	Fe	Ni	Cr	Mn	V	Zr	B	Ba	Be	La	Sc	Sr	Y	Ca	Mg	Ti	Na
Na	.26	.90	.16	.38	.29	0	0	.61	0	.53	0	.23	.58	.53	.79	.22	.27	.28	0	
Ti	0	-.23	0	0	.28	0	0	.29	.27	0	0	0	0	.22	0	0	0	0		
Mg	0	0	0	.31	0	-.31	0	0	.22	.24	.33	0	.23	0	.33	0	.67			
Ca	0	0	0	0	.29	-.26	.29	.23	.46	0	0	0	0	0	.32	0				
Y	0	0	0	0	0	0	0	0	0	0	0	0	.35	.72	.32					
Sr	.48	.70	.31	.50	.36	-.33	0	.62	0	.52	.39	.38	.73	.56						
Sc	0	.37	.28	.28	.24	0	0	.55	0	.25	0	0	.64							
La	.34	.49	.35	.43	.31	.22	0	.62	0	.43	.38	0								
Be	.36	.31	0	0	0	0	0	0	-.24	.22	0									
Ba	0	0	.25	.26	0	-.41	0	0	.21	0										
B	.25	.40	0	.24	.24	0	0	.40	0											
Zr	-.25	0	0	0	0	0	0	0												
V	.36	.49	.40	.62	.44	0	0													
Mn	.24	0	0	0	0	0														
Cr	0	-.24	0	0	0															
Ni	.39	.24	.62	.22																
Fe	.45	.34	0																	
Mo	0	0																		
Pb	.30																			

Correlation Coefficient Matrix

High Silica Zone

Figure 25. High-silica alteration zone correlation coefficient matrix.

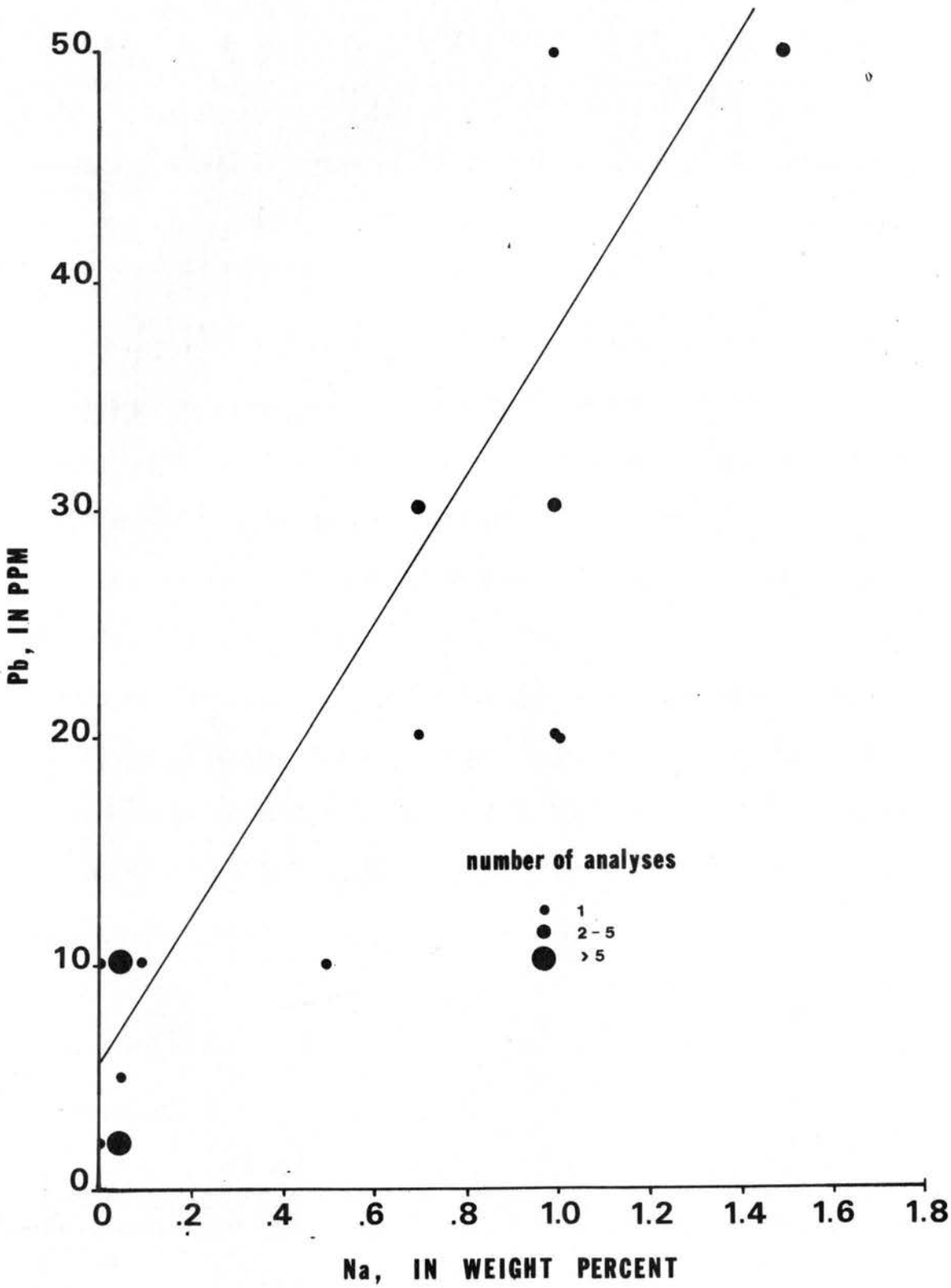

Figure 26. Pb-Na plot showing linear relationship demonstrated by these elements in rocks of the high-silica alteration zone.

for rocks of the high-silica alteration zone, against Pb, however, demonstrates an excellent linear relationship (Fig. 27). Therefore, the close covariation of these elements indicates that the behavior of Pb in the high-silica alteration zone is primarily lithophile in character.

Plots of Pb and Na against SiO_2[1] demonstrate good inverse linear relationships (Fig. 28). Evidently, the strong correlations exhibited by Pb and Na reflect the hydrolytic decomposition of feldspars by the invading hydrothermal solutions.

It has been shown that the dominant alteration process in the high-silica alteration zone is the hydrolytic decomposition of the silicate minerals and the resultant base cation leaching such that SiO_2 is the ultimate alteration product. Other elements that exhibit positive correlation coefficients in Fig. 25 (e.g. Ca, Sr, La, and Fe) also demonstrate inverse linear relationships with SiO_2, and in so doing, nicely illustrate the above mentioned process.

If Mo had been introduced with the invading hydrothermal solutions, negative values of correlation coefficients with the lithophile elements would be expected. To the contrary, Mo demonstrates positive coefficient values with Na, Sr, Sc, La, Ba, V, and Ni. However, this apparent contradiction can be explained in terms of the distribution

---

[1] SiO_2 was determined by calculating oxide weight percents from the emission spectrographic analyses of Al, Ti, Fe, Mg, Ca, Na, and K; and subtracting from 100.

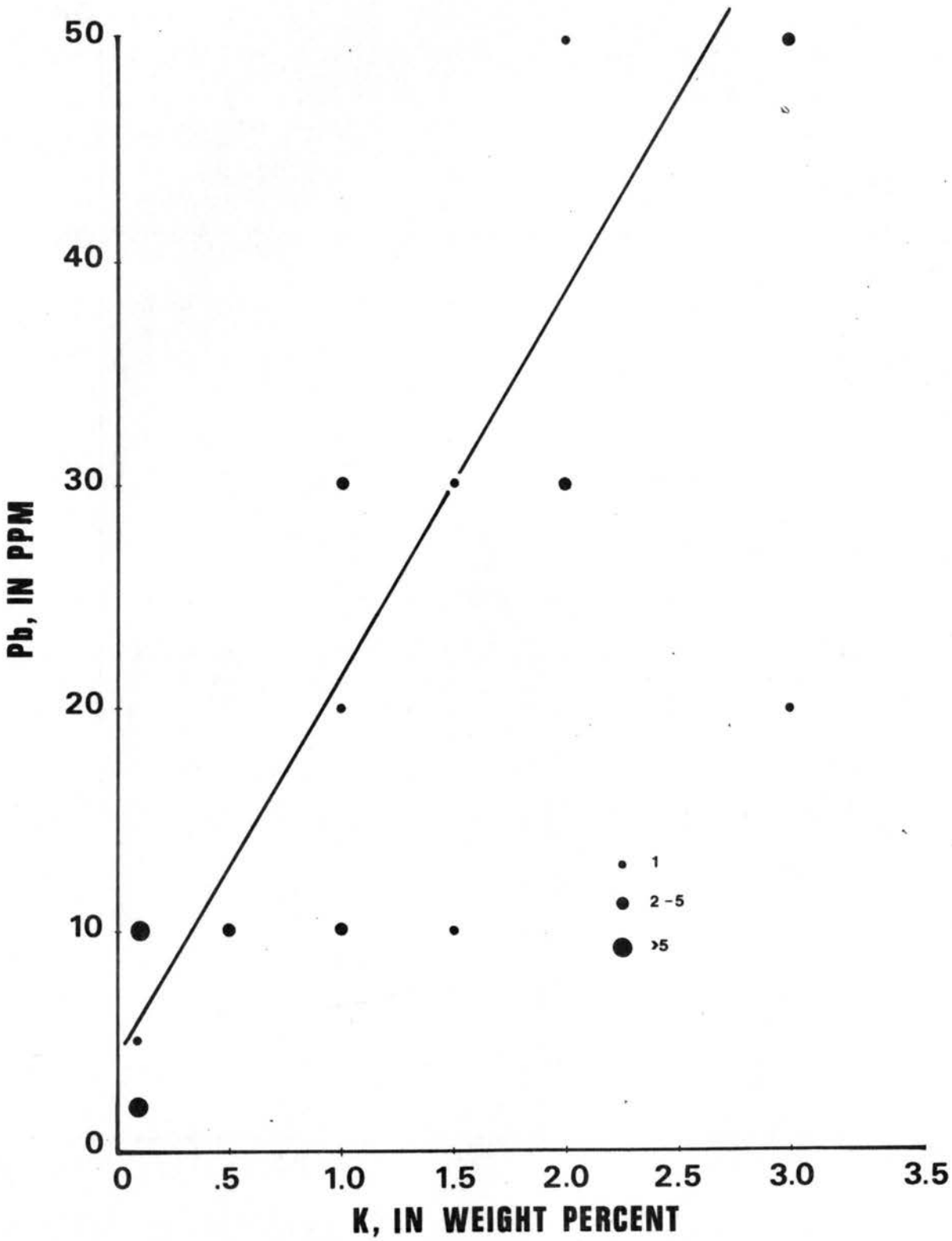

Figure 27. Pb-K plot showing linear relationship demonstrated by these elements in rocks of the high-silica alteration zone.

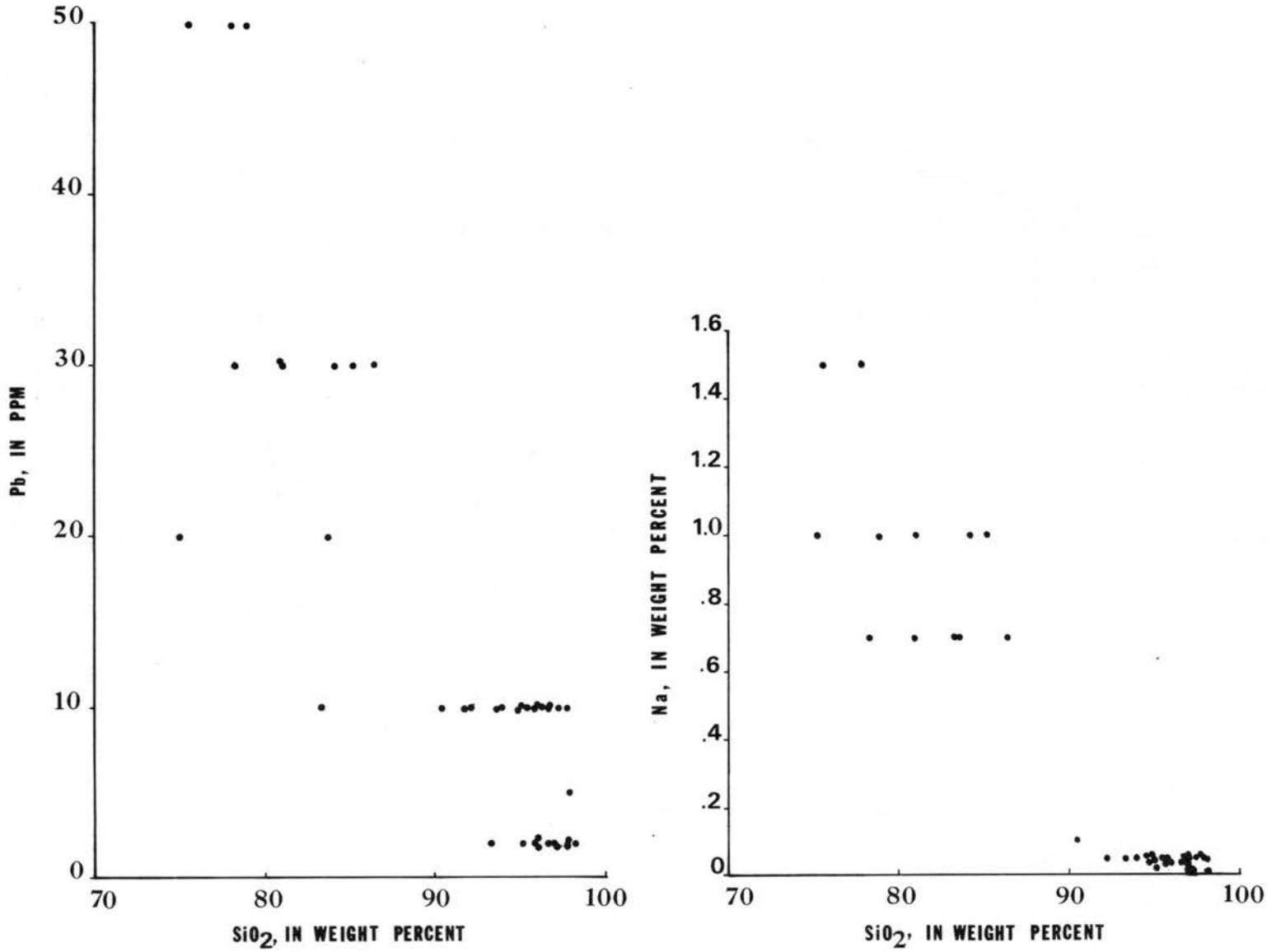

Figure 28. Plots of Pb and Na against SiO_2 reflecting the hydrolytic decomposition of feldspars.

of the anomalous Mo values. Highest concentrations of Mo in rocks from the high-silica zone are restricted to vuggy cavernous samples. Chemical analyses indicate that the dense jasperoidal rocks generally have a higher SiO_2 content than do the vuggy, cavernous high-silica zone samples. The chalcophile nature of Mo, as a result, is camouflaged, and its geochemical behavior is not distinguished from that of the lithophile elements.

Correlation Coefficient Matrix for the Advanced Argillic Alteration Zone

The matrix in Fig. 29 is based on 86 emission spectrographic analyses. It is very difficult to discern geochemically meaningful relations among various elements in this matrix. Two factors may serve to dilute or confuse the geochemical relations with respect to the geochemistry of this alteration zone: (1) Since the distinction between the high-silica and advanced argillic alteration zones is somewhat arbitrary, rocks from these zones are widely varied in composition and extent of alteration; (2) Even though the highest values for various elements (Cu, Pb, Zn) occur in the advanced argillic zone, these rocks demonstrate an overall tendency to be depleted of these elements with respect to unaltered rocks.

Zn exhibits positive correlation coefficient values with Mn, Ni, and Co. The geochemistry of Zn is discussed in some detail in the discussion of the silicified quartz latite matrix (Fig. 30). Briefly,

	Cu	Pb	Zn	Mo	Fe	Ni	Co	Cr	Mn	V	Zr	B	Ba	Be	La	Sc	Sr	Y	Ca	Mg	Ti
Na	0	.53	.43	0	0	.24	0	0	.30	0	0	0	.44	.37	.19	0	0	.28	.58	.45	0
Ti	0	0	0	0	0	0	0	.23	0	.24	0	0	0	0	0	36	.40	0	0	0	
Mg	0	0	0	0	0	0	0	0	0	0	0	0	0	0	0	.21	0	0	.20		
Ca	0	.30	.52	0	0	.30	.20	0	.43	0	0	0	.40	.37	0	.20	0	.30			
Y	0	.24	.39	0	0	0	0	0	.38	.27	0	0	.46	0	.45	.51	0				
Sr	.29	0	0	0	0	0	0	-.21	0	.45	-.28	0	0	37	.19	.47					
Sc	.37	0	.23	0	0	0	0	0	0	.59	0	0	38	.24	.31						
La	0	38	0	0	0	0	0	0	0	0	34	0	41	0							
Be	.35	.31	.43	0	0	.51	.25	-.20	.20	.38	-.38	.21	0								
Ba	0	.28	.28	0	0	0	0	0	0	.18	0	0									
B	.18	.19	0	0	0	0	0	-.21	0	.21	0										
Zr	.20	0	0	0	-.21	.27	0	.23	0	0											
V	.49	0	.20	0	44	.30	28	-.19	0												
Mn	0	.29	.76	0	0	.35	.48	0													
Cr	.24	-.19	0	0	0	0	0														
Co	.37	.22	.58	0	0	.64															
Ni	.27	0	.49	-.18	0																
Fe	.55	.26	0	.65																	
Mo	.27	0	0																		
Zn	.23	.34																			
Pb	0																				

Advanced Argillic Zone
Correlation Coefficient Matrix

Figure 29. Advanced argillic alteration zone correlation coefficient matrix.

	Cu	Pb	Zn	Mo	Fe	Ni	Co	Cr	Mn	V	Zr	B	Ba	Be	La	Sc	Sr	Y	Ca	Mg	Ti
Na	0	.43	0	0	0	0		0	0	0	0	0	.57	0	0	0	0	0	0	.69	0
Ti	.51	0	.63	0	.55	.53	-	0	.66	.56	0	0	0	0	0	.63	0	0	0	0	
Mg	0	0	66	0	0	.50	-	0	.79	0	0	0	.51	0	0	.66	0	0	0		
Ca	.64	0	0	0	.44	0		0	0	0	0	0	0	.49	0	0	.47	.65			
Y	.69	0	0	0	0	0	-	0	0	0	0	0	.50	0	.63	0	0				
Sr	0	0	0	0	0	0	-	0	0	0	0	0	0	.71	0	0					
Sc	0	0	1.0	0	.71	.73	-	0	.95	0	0	0	0	0	0						
La	.43	0	0	0	0	0	-	0	0	0	.53	.58	.43	0							
Be	0	0	0	-46	0	0	-	0	0	43	0	0	0								
Ba	0	0	0	0	0	0	-	0	0	0	0	0									
B	0	-60	0	.69	0	0	-	0	0	0	0										
Zr	0	0	0	.44	0	0	-	-45	0	0											
V	0	0	0	0	0	.45	-	0	0												
Mn	0	0	.95	0	.58	.71	-	0													
Cr	0	0	0	0	0	0	-														
Co	-	-	-	-	-	-															
Ni	0	0	.73	0	.72																
Fe	.62	0	.71	0																	
Mo	0	0	0																		
Zn	0	0																			
Pb	0																				

Silicified $Tqlp_1$

Correlation Coefficient Matrix

Figure 30. Silicified quartz latite alteration zone correlation coefficient matrix.

Zn, Mn, Ni, and Co each substitute for Mg and ferrous Fe in ferromagnesian silicate minerals. Evidently, Zn was not introduced by the hydrothermal solutions, and its concentration in the advanced argillic rocks is dominantly a function of the extent to which ferromagnesian minerals were decomposed and the degree to which Zn was subsequently leached from the altered rocks.

Pb is most strongly correlated with Na in the matrix for the advanced argillic alteration zone. The concentration of Pb in the advanced argillic rocks must be a function of the degree of decomposition of potash-bearing silicate minerals and the mobility of Pb after its liberation.

The chalcophile nature of Mo is weakly reflected in Fig. 29. Mo exhibits positive correlation coefficient values with only Fe and Cu. Mo, Fe, and Cu probably all occur as sulfide minerals in the advanced argillic assemblage.

Correlation Coefficient Matrix for the Silicified Quartz Latite Alteration Zone

The correlation coefficient matrix for silicified quartz latitic rocks (Fig. 30) is based on 16 analyses. Several of the elements demonstrate excellent linear correlation coefficient values that allow some useful geochemical interpretations regarding the nature of the altering hydrothermal solutions.

Most conspicuous are a group of six elements--Mg, Zn, Fe, Mn, Ni, and Sc--all of which exhibit positive correlation values

greater than 0.70. The behavior of Zn, Sc, Mn, and Ni is each closely related to the geochemistry of magnesium and ferrous iron. Because of similar ionic radii, each of the former elements is capable of isomorphous substitution for Mg^{+2} and Fe^{+2} in many ferromagnesian silicate minerals. The governing factor in atomic substitution is the size of the ions and it is not essential that the substituting ions have exactly like charges (Mason, 1966). The ionic radii of these elements are compared below:

Sc^{+3} 0.83Å, Mg^{+2} 0.78Å, Ni^{+2} 0.78Å, Mn^{+2} 0.80Å, Fe^{+2} 0.83Å, Zn^{+2} 0.83Å.

The elements Fe, Ni, Mn, Sc, and Mg usually are not strongly fractionated to residual fluids during magmatic crystallization. It is apparent, by the strong linear relationship Zn exhibits with each of these elements that its abundance in the silicified quartz latites is entirely determined by the degree to which it has substituted for Mg and Fe in the crystal lattices of the biotite and hornblende crystals in the quartz latitic rocks.

Pb is most highly correlated with Na. The Pb content in these rocks is apparently a function of the degree to which Pb has isomorphously replaced K in potassic silicate minerals.

SUMMARY AND CONCLUSIONS

GEOLOGIC HISTORY

The oldest rocks exposed in the study area are flows and breccias belonging to the Conejos Formation. Ash-flow tuffs, representing the second stage of volcanism in the San Juan Mountains, do not extend into the thesis area. The final episode of volcanic activity is characterized by olivine basaltic andesite flows; silicic flow-banded rhyolite dikes; and small, hybridized dikes.

The first evolutionary stage of Tertiary San Juan volcanism is characterized by large volumes of intermediate lavas and breccias. These rocks, members of the Conejos Formation, have been mapped as four discrete units according to texture, composition, and stratigraphic position. Field relations indicate that the Conejos volcanics originated from numerous local centers. Early quartz latites were derived from a small, silicified plug in the northeastern corner of the study area. Andesitic and mafic quartz latitic lavas were apparently derived from a center northwest of the study area, and rhyodacitic lavas were derived from a center south of the mapped area.

The second episode of volcanism in the San Juan Mountains is represented by a series of ash-flow tuffs. There are no exposures of pyroclastic rocks in the study area, however, a small granodiorite stock intrudes andesitic and rhyodacitic flows of the Conejos Formation

and may be equivalent in age to ash-flow tuffs, exposed farther to the west. Associated with the granodioritic stock are small discontinuous outcroppings of quartz monzonite, and a small mafic dike that may have been co-magmatic with the granodioritic rocks.

Late-stage volcanism in the San Juan region is characterized by a bimodal association of alkali olivine basaltic andesite and silicic alkali rhyolites. Mixed lava complexes, where rhyolitic and basaltic lavas have intermingled, are also distinctive of the final episode of volcanism. Based on composition and stratigraphic position, basaltic olivine andesite flows on the western and in the central portions of the study area have been mapped as part of the Hinsdale Formation, and are believed to be representatives of the latest San Juan volcanic activity. Small, hybridized dikes, commonly with an assortment of phenocrysts, crop out in the study area and are vestiges of the late-stage activity.

Faults in the study area tend to be short, and straight or gently curved. Angular breaks and branch faults are common. Steeply-dipping normal faults, or vertical faults, commonly are associated with or bound small horst and graben structures. Field relations indicate histories of recurrent movement, with the latest activity associated with regional crustal extension and the development of the Rio Grande Rift.

All of the Conejos Formation lavas show some hydrothermal alteration effects. The mafic granodiorite stock is unaltered, except along its northern border, where it is in contact with early intermediate andesitic lavas. Lavas and intrusives of the late bimodal association have not been affected by the hydrothermal solutions. Therefore, it is apparent that the mineralizing and altering solutions must have been introduced concomitantly with, or shortly after emplacement of the granodiorite intrusive.

SUGGESTIONS FOR FURTHER EXPLORATION

Early day prospectors, in the search for gold, left their mark on the Tracy Canyon area. The area is dotted by small exploration pits where bright orange and red iron oxides, black manganese oxides, and occasional iridescent oxide surface coatings aroused the explorer's curiosities. In the south-central part of the thesis area, two vertical shafts and a long since caved adit are the testimony to some of the more ambitious of these prospectors. There was no recorded production from any of these workings and no surficial mineralization of economic significance has been recognized.

In 1969, W. A. Bowes and Associates of Steamboat Springs, Colorado located 84 claims which included most of the altered rocks in the area. As the claims were being staked, a detailed soil geochemistry survey was conducted on a grid system and a reconnaissance geologic map was compiled. In addition, three short (15-26 meters) test diamond drill holes were placed in the jasperoid breccia targets.

The irregular alteration and the geochemical characteristics associated with the breccia pipes in the Tracy Canyon area are typical of the alteration pattern and geochemistry of breccia pipes in other mining districts (Fisher and Leedy, 1973; Armbrust, 1969; Perry, 1961; and Barrington and Kerr, 1961). In addition to being important

producers of sulfide minerals, mineralized breccia pipes are significant because they are often closely related to large orebodies, most notable are the porphyry copper-molybdenum deposits. No intrusives, demonstrating a close affinity with the jasperoid breccia pipes, have been identified in the study area. This could imply the existence of a deep-seated intrusive which might be a possible porphyry copper-molybdenum exploration target. The nature of the alteration and geochemistry, overall, is not consistent with the porphyry ore deposit model (Lowell and Gilbert, 1970), however, and it is unlikely that a subsurface orebody of this nature exists.

The most likely targets for further exploration in the Tracy Canyon area are, therefore, the mineralized breccia pipes. None of the three test drill holes, placed in the breccia pipe targets, have penetrated unaltered volcanics. Further exploration and drilling could reveal economic concentrations of molybdenum and/or gold in the breccia pipes in deposits similar to the breccia pipe deposits of the Red Mountain district, northwest San Juan Mountains, Colorado (Fisher and Leedy, 1973).

REFERENCES CITED

Ahrens, L. H., editor, 1968, Origin and Distribution of the Elements: Pergamon Press, New York, 1178 p.

Armbrust, G., 1969, Hydrothermal Alteration of a Breccia Pipe Deposit: Econ. Geol., v. 64, p. 551-563.

Bailey, E. H., and Stevens, R. E., 1960, Selective staining of K-feldspar and plagioclase on rock slabs and thin sections: Amer. Mineralogist, v. 45, p. 1020-1025.

Barrington, J., and Kerr, P. F., 1961, Breccia Pipe near Cameron, Arizona: Geol. Society of America Bull., v. 74, p. 1405-1410.

Beverly, C. E., 1969, The petrology and structure of Precambrian crystalline and Tertiary igneous rocks in the northeast quarter of the Rustic quadrangle, Larimer County, Colorado: unpublished M.S. Thesis, Colorado State University, 99 p.

Bruns, D. L., Epis, R. C., Weimer, R. J., and Steven, T. A., 1971, Stratigraphic relations between Bonanza Center and adjacent parts of the San Juan Volcanic Field south-central Colorado: New Mexico Geol. Society, twenty-second field conf, p. 183-190.

Christiansen, R. L., and Lipman, P. W., 1972, Late Cenozoic, pt. 2 of Cenozoic volcanism and plate tectonic evolution of the Western United States: Royal Soc. London Philos. Trans., vol. 271, p. 249-284.

Fisher, F. S., and Leedy, W. P., 1973, Geochemical Characteristics of Mineralized Breccia Pipes in the Red Mountain District, San Juan Mountains, Colorado: U.S. Geol. Survey Bull. 1381, 43 p.

Goldschmidt, V. M., 1958, Geochemistry: Muir, editor, Oxford University Press, New York, 730 p.

Hawkes, H. E. and Webb, J. S., 1962, Geochemistry in Mineral Exploration: Harper and Row, New York, 415 p.

Hemley, J. J., and Jones, W. R., 1964, Chemical aspects of hydrothermal alteration with emphasis on hydrogen metasomatism: Econ. Geol., v. 59, no. 4, p. 538-569.

James, H. L., editor, 1971, Guidebook of the San Luis Basin, Colorado: New Mexico Geol. Society, twenty-second field conference, 325 p.

Kerr, P. F., 1959, Optical Mineralogy: McGraw-Hill Inc., New York, 442 p.

Kittleman, L. R., Jr., 1963, Glass Bead Silica Determination for a Suite of Volcanic Rocks from the Owyhee Plateau, Oregon: Geol. Society of America Bull., v. 74, p. 1405-1410.

Krauskopf, K. B., 1967, Introduction to Geochemistry: McGraw-Hill Inc., New York, 721 p.

Krumbein, W. C., and Graybill, F. A., 1965, An Introduction to Statistical Models in Geology: McGraw-Hill Inc., New York, 475 p.

Larsen, E. S., Jr., and Cross, W., 1956, Geology and Petrology of the San Juan region, southwestern Colorado: U.S. Geol. Survey Prof. Paper 258, 303 p.

Lipman, P. W., 1975, Evolution of the Platoro Cauldera Complex and Related Volcanic Rocks, Southeastern San Juan Mountains, Colorado: U.S. Geol. Survey Prof. Paper 852, 128 p.

Lipman, P. W., Steven, T. A., and Mehnert, H. H., 1970, Volcanic history of the San Juan Mountains, Colorado, as indicated by potassium-argon dating: Geol. Society of America Bull., v. 81, p. 2329-2352.

Lipman, P. W., Mutscher, F. E., Bryant, B., and Steven, T. A., 1969, Similarity of Cenozoic igneous activity in the San Juan and Elk Mountains, Colorado, and its regional significance: U.S. Geol. Survey Prof. Paper 650-D, p. D33-D42.

Lipman, P. W., 1968, Geology of Summer Coon Volcanic Center, Eastern San Juan Mountains, Colorado: Colo. Sch. Mines Quart., v. 63, no. 3, p. 211-236.

Lovering, T. G., 1972, Jasperoid in the United States--Its Characteristics, Origin, and Economic Significance: U.S. Geol. Survey Prof. Paper 710, 164 p.

Lowell, D. J., and Guilbert, J. M., 1970, Lateral and Vertical Alteration-Mineralization Zoning in Porphyry Ore Deposits: Econ. Geol., v. 65, no. 4, p. 373-407.

Perry, V. D., 1961, The Significance of Mineralized Breccia Pipes: Mining Eng., April, p. 367-376.

Steven, T. A., Lipman, P. W., Hail, W. J., Jr., Barker, F., and Luedke, R. G., 1974, Geologic Map of the Durango Quadrangle, Southwestern Colorado: U.S. Geol. Survey Map I-764.

Steven, T. A., and Epis, R. C., 1968, Oligocene volcanism in south-central Colorado: Colorado School of Mines Quart., v. 63, no. 3, p. 241-258.

Samuelson, D. R., 1971, Petrology and structure of Precambrian crystalline and Tertiary igneous rocks, Manhattan district, Larimer County, Colorado: unpublished M.S. thesis, Colorado State University, 89 p.

Williams, H., Turner, F. J., and Gilbert, C. M., 1954, Petrography, an introduction to the study of rocks in thin sections: W. H. Freeman and Co., San Francisco, 406 p.

APPENDIX

GENERAL STATEMENT

Two hundred-eighty rock chip samples were collected while in the field for geochemical analyses. Semiquantitative spectrographic analyses for 35 elements were generously provided by W. A. Bowes and Associates, Steamboat Springs, Colorado.

Analysis results for Cu, Pb, Zn, Mo, and As are presented in Table A-1. N denotes not detected. L indicates an element was detected, but was below the limit of determination. The lower limit of determination for Cu, Pb, Zn, Mo, and As is given below:

Cu	Pb	Zn	Mo	As
5 ppm	10 ppm	200 ppm	5 ppm	200 ppm

Table A-1. Bedrock chip samples (values are in parts per million).

Sample	Rock Type	Cu	Pb	Zn	Mo	As
1	High Silica	10	30	N	N	N
2	High Silica	15	L	N	N	N
3	Silic. $Tqlp_1$	15	70	N	N	N
4	$Tqlp_1$	20	20	N	N	N
5	Adv. Arg.	30	10	N	N	N
6	Adv. Arg.	20	20	N	N	N
7	Adv. Arg.	30	20	N	N	N
8	Adv. Arg.	30	30	N	N	N
9	Adv. Arg.	20	20	N	N	N
10	$Tqlp_2$	20	30	N	N	N
11	Adv. Arg.	60	20	N	N	N
12	Adv. Arg.	20	20	N	N	N
13	Tap	20	30	N	N	N
14	Tap	30	30	N	N	N
15	Adv. Arg.	60	30	N	N	N
16	Adv. Arg.	30	30	N	N	N
17	Adv. Arg.	20	20	N	N	N
18	Adv. Arg.	50	20	N	N	N
19	Adv. Arg.	30	10	N	N	N
20	High Silica	20	10	N	N	N
21	High Silica	50	10	N	N	N
22	High Silica	50	N	N	N	N
23	High Silica	10	N	N	N	N
24	High Silica	15	10	N	N	N
25	Adv. Arg.	40	10	N	N	N
26	Adv. Arg.	30	10	N	N	N
27	Adv. Arg.	20	10	N	N	N
28	Adv. Arg.	20	20	N	N	N
29	Adv. Arg.	20	10	N	N	N
30	High Silica	10	N	N	N	N
31	$Tqlp_1$	10	30	L	N	N
35	High Silica	20	N	N	N	N
36	High Silica	30	N	N	N	N
37	High Silica	30	10	N	N	N
38	Adv. Arg.	20	20	N	N	N
39	High Silica	30	30	N	N	N
42	Tap	70	20	200	N	N
43	Adv. Arg.	200	10	L	N	N

Sample	Rock Type	Cu	Pb	Zn	Mo	As
45	Tap	50	10	L	N	N
46	High Silica	30	N	N	N	N
47	High Silica	70	30	N	N	N
48	High Silica	30	20	N	N	N
49	Silic. $Tqlp_1$	20	30	N	N	N
50	High Silica	30	30	N	N	N
51	Silic. $Tqlp_1$	20	30	N	N	N
52	Adv. Arg.	15	20	N	N	N
53	High Silica	10	N	N	N	N
54	Silic. $Tqpl_1$	10	30	N	N	N
55	High Silica	30	10	N	N	N
58	Silic. $Tqlp_1$	15	30	N	N	N
60	High Silica	15	30	N	N	N
61	High Silica	15	10	N	N	N
63	High Silica	20	10	N	N	N
64	High Silica	30	10	N	N	N
65	High Silica	15	10	N	N	N
66	Adv. Arg.	20	30	N	N	N
67	High Silica	20	10	N	N	N
68	Adv. Arg.	20	10	N	N	N
69	Adv. Arg.	20	10	N	N	N
70	$Tqlp_1$	10	20	N	N	N
71	High Silica	10	10	N	N	N
72	High Silica	10	N	N	N	N
73	High Silica	30	30	N	L	N
74	High Silica	15	N	N	N	N
75	High Silica	10	N	N	N	N
76	High Silica	15	N	N	N	N
77	High Silica	30	30	N	N	N
78	High Silica	15	N	N	10	N
79	High Silica	15	N	N	5	N
80	High Silica	10	N	N	5	N
81	High Silica	20	N	N	L	N
82	Adv. Arg.	15	N	N	20	N
83	High Silica	20	N	N	L	N
84	Adv. Arg.	30	50	N	10	N
85	Adv. Arg.	15	50	N	L	N
86	$Tqlp_1$	20	30	N	L	N
87	Adv. Arg.	20	N	N	5	N
88	Tap	30	20	N	L	N
89	High Silica	20	10	N	50	700
90	Adv. Arg.	20	20	N	L	N
91	High Silica	20	10	N	N	N

Sample	Rock Type	Cu	Pb	Zn	Mo	As
92	$Tqlp_1$	20	20	N	L	N
93	Adv. Arg.	30	10	N	N	N
94	Adv. Arg.	20	20	N	N	N
95	Adv. Arg.	30	10	N	N	N
96	Tap	20	20	N	N	N
97	Adv. Arg.	30	10	N	N	N
98	$Tqlp_1$	30	20	N	N	N
99	$Tqlp_1$	15	30	N	N	N
100	Adv. Arg.	10	10	N	N	N
101	Adv. Arg.	10	L	N	N	N
102	Adv. Arg.	30	10	N	N	N
103	Tgrdi	20	10	N	N	N
104	Tba	50	10	L	N	N
105	Adv. Arg.	50	20	N	N	N
106	$Tqlp_1$	15	50	N	N	N
107	Tap	50	20	L	N	N
108	Tap	20	30	L	N	N
109	Adv. Arg.	60	20	L	N	300
110	$Tqlp_1$	60	20	200	N	N
112	$Tqlp_1$	20	40	N	N	N
113	Tqmp	20	20	N	N	N
114	Tqmp	15	30	N	N	N
115	Adv. Arg.	60	20	N	200	1500
116	Adv. Arg.	10	10	N	N	N
117	Adv. Arg.	50	30	N	N	N
118	Adv. Arg.	30	50	N	N	N
119	Adv. Arg.	100	70	N	100	1500
121	High Silica	30	20	N	N	N
122	High Silica	20	10	N	N	N
123	Adv. Arg.	20	30	N	N	N
124	High Silica	40	30	N	100	L
125	$Tqlp_1$	20	50	N	N	N
126	High Silica	30	30	N	N	N
129	$Tqlp_2$	20	30	N	N	N
130	Adv. Arg.	70	30	N	100	N
131	Tba	100	30	N	N	N
132	Tap	50	20	N	N	N
133	Tap	100	30	N	N	N
134	Tgrd	70	30	N	N	N
135	Adv. Arg.	30	30	N	N	N
136	Tap	50	30	N	N	N
137	Adv. Arg.	30	70	N	N	N
138	Tap	30	50	N	N	N

Sample	Rock Type	Cu	Pb	Zn	Mo	As
139	Tgrd	40	30	N	N	N
140	Tap	50	30	N	N	N
142	Tap	5	10	N	N	N
143	Tap	15	20	N	N	N
144	Adv. Arg.	10	10	N	10	N
145	$Tqlp_1$	20	10	N	N	N
147	Tba	50	10	N	N	N
148	Tap	30	10	N	N	N
149	Adv. Arg.	60	20	N	N	N
150	Tap	20	10	N	N	N
151	Silic. $Tqlp_1$	15	20	N	5	N
152	Adv. Arg.	50	10	N	N	N
153	Tap	5	20	N	N	N
154	Adv. Arg.	20	20	N	L	N
155	High Silica	20	10	N	N	N
157	Adv. Arg.	70	10	N	20	N
158	Tap	50	10	N	N	N
159	Adv. Arg.	20	30	N	N	N
160	High Silica	20	10	N	N	N
161	Adv. Arg.	15	20	N	N	N
162	Adv. Arg.	15	10	N	N	N
163	Adv. Arg.	5	N	N	N	N
164	Adv. Arg.	20	10	N	N	N
165	Adv. Arg.	20	10	N	N	N
166	Adv. Arg.	15	N	N	N	N
167	High Silica	15	N	N	N	N
168	High Silica	20	30	N	N	N
169	Adv. Arg.	10	10	N	N	N
170	Adv. Arg.	20	20	N	N	N
171	Silic. $Tqlp_1$	15	15	N	N	N
172	Silic. $Tqlp_1$	15	30	N	N	N
173	Silic. $Tqlp_1$	15	30	N	N	N
174	Silic. $Tqlp_1$	20	50	N	N	N
175	$Tqlp_1$	15	50	N	N	N
176	$Tqlp_1$	15	50	200	N	N
177	Tap	100	30	200	N	N
179	Adv. Arg.	50	30	N	N	N
180	High Silica	20	10	N	N	N
181	High Silica	30	10	N	N	N
182	Adv. Arg.	30	20	N	N	N
183	High Silica	15	N	N	N	N
184	Adv. Arg.	50	30	N	N	N
185	Tap	50	30	200	N	N

Sample	Rock Type	Cu	Pb	Zn	Mo	As
186	High Silica	15	10	N	N	N
187	High Silica	15	10	N	N	N
188	High Silica	20	10	N	N	N
189	High Silica	30	10	N	N	N
190	High Silica	20	20	N	5	N
191	$Tqlp_1$	20	30	200	5	N
192	Tap	40	30	200	5	N
193	Adv. Arg.	20	50	L	N	N
195	Adv. Arg.	15	50	N	N	N
196	Tap	40	20	L	5	N
197	Adv. Arg.	20	50	N	N	N
198	High Silica	20	10	N	L	N
199	Tb_{hy}	30	30	L	L	N
200	$Tqlp_1$	20	50	N	L	N
201	$Tqlp_1$	15	50	L	L	N
202	Adv. Arg.	20	10	N	5	N
203	Adv. Arg.	15	50	L	N	N
204	High Silica	15	10	N	10	N
205	Tap	50	20	200	10	N
206	Adv. Arg.	20	10	N	10	N
207	Adv. Arg.	10	10	N	5	N
208	Adv. Arg.	30	50	N	L	N
209	Adv. Arg.	20	50	N	L	N
210	Adv. Arg.	20	20	N	100	N
211	Adv. Arg.	20	50	N	N	N
212	High Silica	20	50	N	N	N
213	Silic. $Tqlp_1$	20	50	N	N	N
214	$Tqlp_1$	50	30	L	N	N
215	High Silica	20	N	N	N	N
216	$Tqlp_1$	20	50	200	L	N
217	High Silica	15	N	N	N	N
218	$Tqlp_1$	60	30	L	L	N
219	Tap	20	30	L	L	N
220	Tap	50	30	L	L	N
221	$Tqlp_1$	10	30	L	L	N
222	High Silica	20	50	N	N	N
223	High Silica	10	N	N	N	N
224	Tap	30	30	1	5	N
225	Tap	50	20	L	5	N
226	Adv. Arg.	50	30	L	5	N
229	Adv. Arg.	50	30	L	5	200
230	Adv. Arg.	100	30	N	5	N
231	Tap	30	50	L	5	N

Sample	Rock Type	Cu	Pb	Zn	Mo	As
232	Tap	50	30	L	5	N
233	$Tqlp_1$	30	30	L	L	N
234	Tr_{hy}	15	30	N	L	N
235	Adv. Arg.	30	30	N	N	N
236	Tap	50	20	L	L	N
237	$Tqlp_1$	43	30	L	L	N
238	$Tqlp_1$	30	30	L	L	N
239	Tr_{hy}	30	30	L	L	N
240	$Tqlp_1$	30	30	L	L	N
241	Silic. $Tqlp_1$	30	20	L	L	N
244	Adv. Arg.	15	30	N	L	N
245	Adv. Arg.	15	50	N	L	N
246	Silic. $Tqlp_1$	40	50	N	L	N
247	High Silica	15	N	N	N	N
248	Silic. $Tqlp_1$	15	50	N	L	N
249	Tb_{hy}	40	30	L	L	N
250	Tb_{hy}	40	30	L	L	N
251	Tb_{hy}	40	30	L	L	N
252	$Tqlp_1$	30	30	L	L	N
253	Adv. Arg.	50	20	L	5	N
254	$Tqlp_1$	20	70	L	N	N
255	Tap	30	30	200	L	N
256	Tap	50	30	L	L	N
260	Tap	40	30	L	L	N
261	Tap	40	30	L	L	N
262	Tap	30	30	L	L	N
263	Tap	50	30	L	L	N
264	Tap	50	30	L	L	N
265	Tap	50	70	L	L	N
266	Tap	40	50	L	L	N
267	Adv. Arg.	15	50	N	N	N
268	Adv. Arg.	30	70	300	L	N
269	Adv. Arg.	50	30	L	L	N
270	Tba	50	30	L	5	N
271	$Tqlp_1$	20	50	N	L	N
272	$Tqlp_2$	30	20	N	L	N
273	Adv. Arg.	30	50	L	L	N
274	Tap	40	50	L	L	N
275	Tap	40	30	L	L	N
276	Tap	40	30	L	L	N
277	Tap	15	30	L	L	N
278	Adv. Arg.	15	30	N	L	N

Sample	Rock Type	Cu	Pb	Zn	Mo	As
279	High Silica	20	50	N	L	N
280	High Silica	30	30	N	L	N
281	Tap	20	30	L	L	N
282	Silic. $Tqlp_1$	20	30	L	L	N
283	Silic. $Tqlp_1$	20	30	N	L	N

PLATE 1

GEOLOGIC AND ALTERATION MAP OF THE TRACY CANYON AREA

Saguache County, Colorado

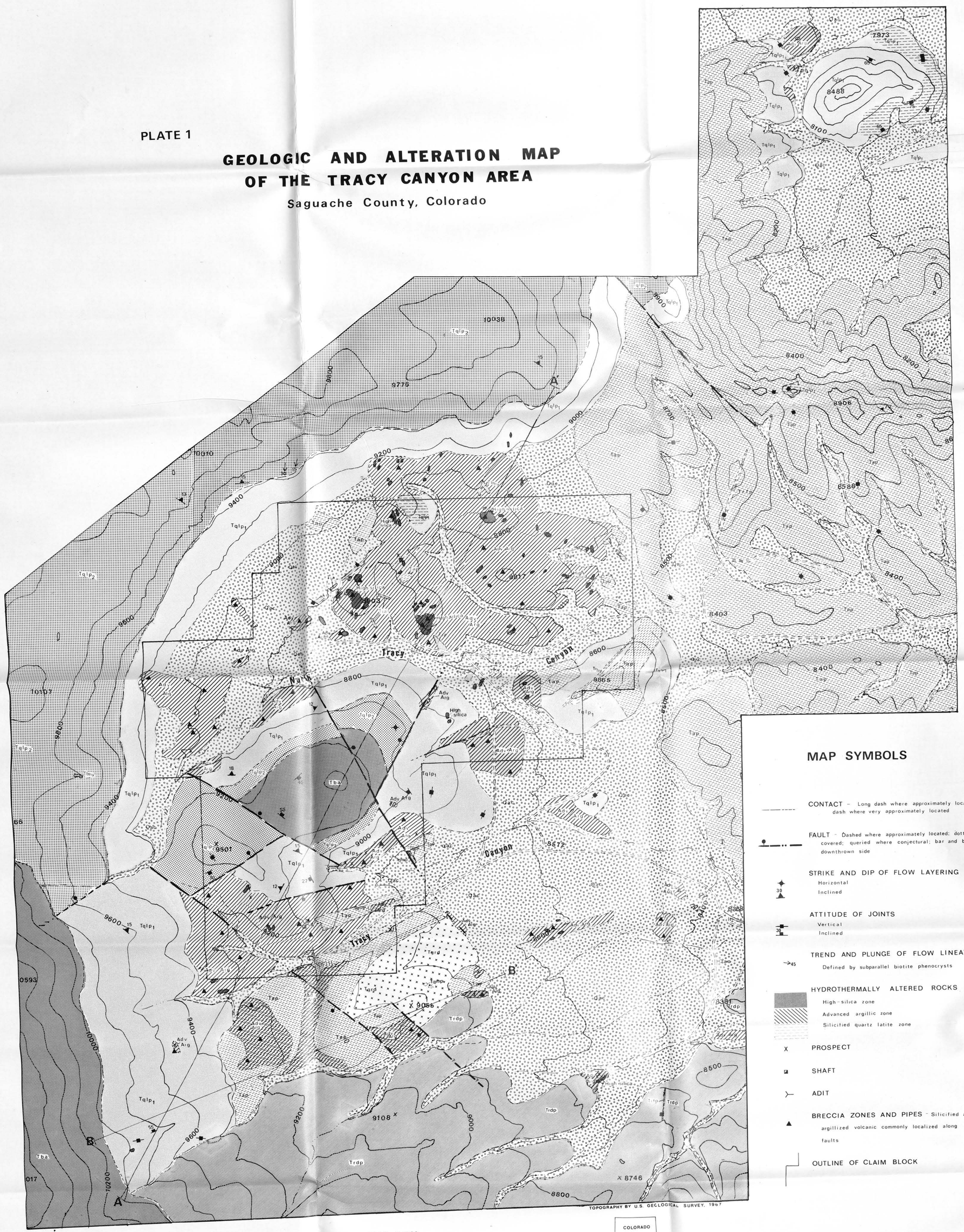

DESCRIPTION OF MAP UNITS

SURFICIAL DEPOSITS

Qac — ALLUVIUM AND COLLUVIUM – Undifferentiated

LAVA UNITS

QUATERNARY

PLIOCENE AND MIOCENE

Thx — HINSDALE FORMATION – Gray porphyritic olivine basaltic andesite flows. Sparse subhedral phenocrysts of olivine largely altered to iddingsite and magnetite

TERTIARY

OLIGOCENE

Trdp — CONEJOS FORMATION – Light gray porphyritic rhyodacite flows, containing 25-40 percent phenocrysts of plagioclase, hornblende, augite, and biotite

Tap — CONEJOS FORMATION – Dark gray porphyritic andesite flows with phenocrysts of plagioclase, biotite, augite, and hypersthene commonly occurring in glomeroporphyritic aggregates

Tqlp2 — CONEJOS FORMATION – Brown to gray porphyritic mafic quartz latite flows and breccias, containing 30-40 percent phenocrysts of plagioclase, biotite, hornblende, augite, hypersthene, and magnetite

Tqlp1 — CONEJOS FORMATION – Purple porphyritic quartz latite flows and breccias with plagioclase, hornblende, and augite (10-15 percent) phenocrysts exhibiting good flow alignment

INTRUSIVE ROCKS

PLIOCENE AND MIOCENE

Trhx — FLOW-BANDED RHYOLITE – Light purple to tan vesicular porphyritic dike with phenocrysts of quartz, sanidine, biotite, and oligoclase

Thy — HYBRIDIZED RHYOLITE – Light purple to brown porphyritic dike near eastern boundary of B.S. claim block. Characterized by corroded sanidine grains and rounded quartz xenocrysts

Thby — HYBRIDIZED BASALTIC ANDESITE – Dark gray to black porphyritic dikes characterized by an assortment of phenocrysts including plagioclase, sanidine quartz, biotite, hornblende, augite, hypersthene, olivine and magnetite

TERTIARY

OLIGOCENE

Tgd — MAFIC GRANODIORITE – Light gray to olive-green medium-grained stock with a hypidiomorphic granular texture

Tgd — HYBRIDIZED MAFIC GRANODIORITE – Light gray intrusive located along a northwest trending fault in the central portion of the study area. The mafic minerals occur in cummulate aggregates and as anhedral rounded blebs

Tia — ANDESITE – Dark gray porphyritic dikes compositionally similar to andesitic flow rocks. Possibly reflect multiple episodes of intrusive activity

Tqmp — QUARTZ MONZONITE – Light gray to tan coarse grained porphyritic rocks occurring as pods and lenses in other intrusives

MAP SYMBOLS

CONTACT – Long dash where approximately located; short dash where very approximately located

FAULT – Dashed where approximately located; dotted where covered; queried where conjectural; bar and ball on downthrown side

STRIKE AND DIP OF FLOW LAYERING
- Horizontal
- 30 Inclined

ATTITUDE OF JOINTS
- Vertical
- 30 Inclined

45 TREND AND PLUNGE OF FLOW LINEATIONS – Defined by subparallel biotite phenocrysts

HYDROTHERMALLY ALTERED ROCKS
- High-silica zone
- Advanced argillic zone
- Silicified quartz latite zone

X PROSPECT

SHAFT

ADIT

BRECCIA ZONES AND PIPES – Silicified and argillized volcanic commonly localized along faults

OUTLINE OF CLAIM BLOCK

N MN 14° — 1962 MAGNETIC DECLINATION

SCALE 1:12000

0 1000 3000 5000 FEET

0 500 1000 METERS

CONTOUR INTERVAL 200 FEET

TOPOGRAPHY BY U.S. GEOLOGICAL SURVEY, 1967

COLORADO ■ Map Location

BY

JAMES W. NEWMAN

1976

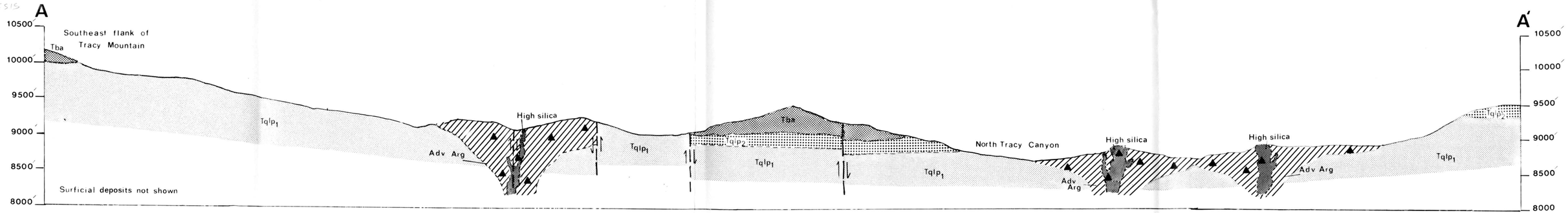

PLATE 2

CROSS-SECTIONS OF THE TRACY CANYON AREA

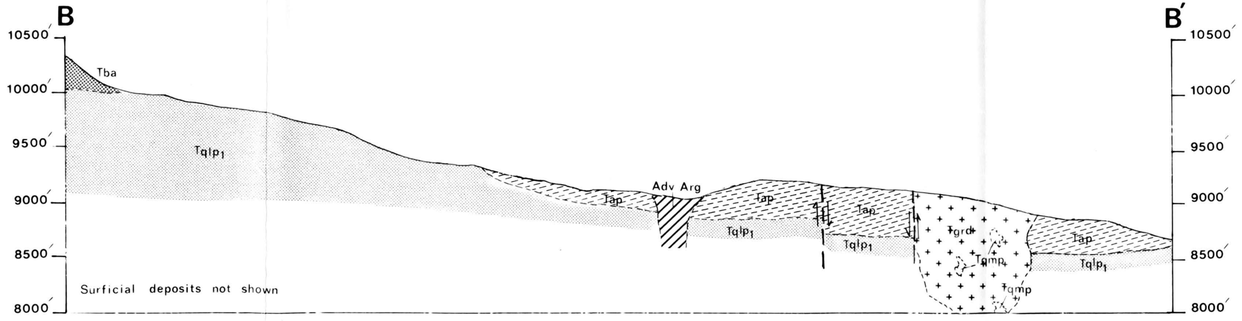

SAMPLE LOCATION MAP

TRACY CANYON AREA

Saguache County, Colorado

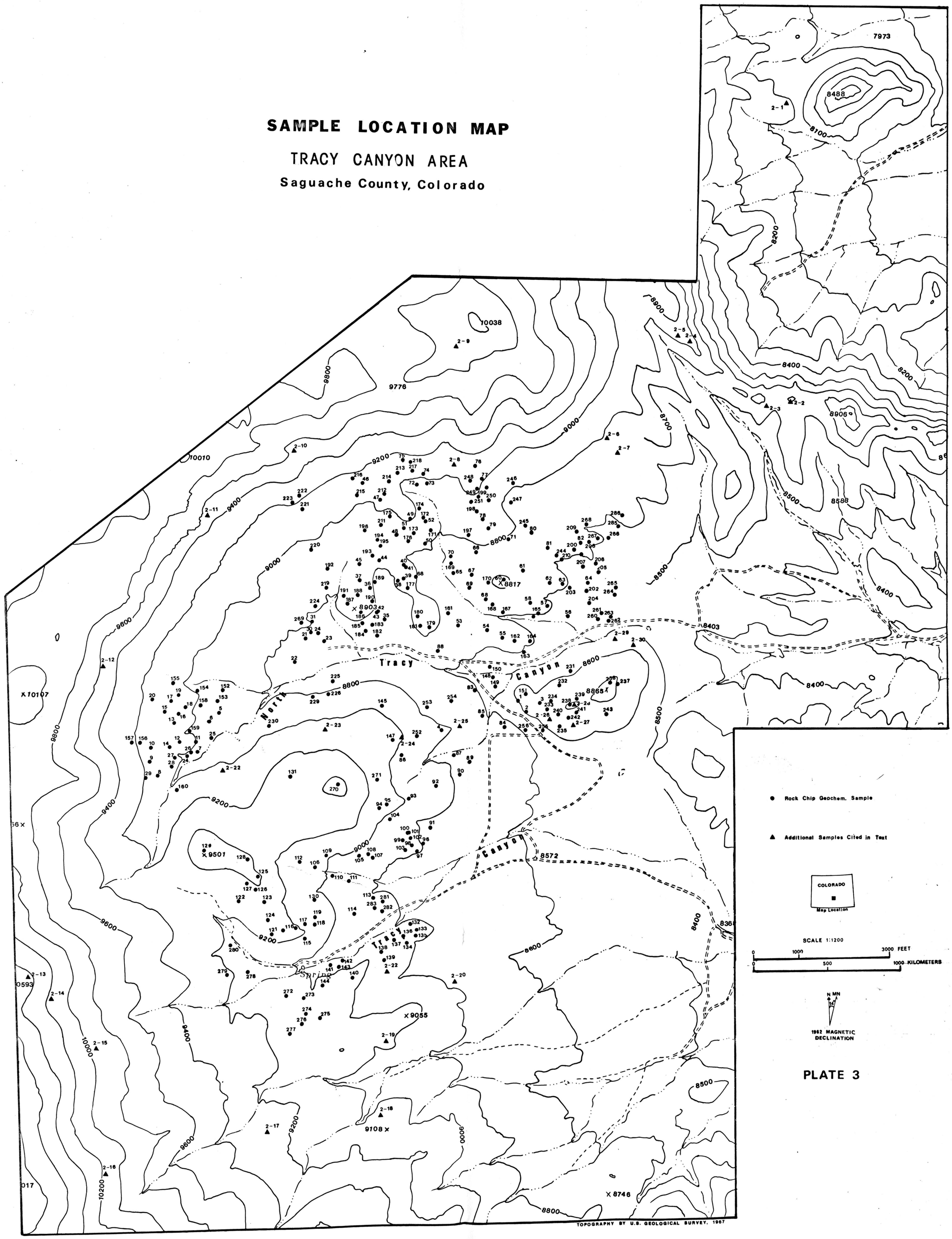

● Rock Chip Geochem. Sample

▲ Additional Samples Cited in Text

COLORADO
■
Map Location

SCALE 1:1200

0 1000 3000 FEET

0 500 1000 KILOMETERS

N MN
14°

1982 MAGNETIC DECLINATION

PLATE 3